Scientific Reports

https://doi.org/10.1038/s41598-026-41336-2

Article in Press

Sleep deprivation alters hippocampal dendritic spines in a contextual fear memory engram

Received: 22 April 2025

Accepted: 19 February 2026

Published online: 24 February 2026

Cite this article as: Tennin M., Matkins H.T., Rexrode L. *et al.* Sleep deprivation alters hippocampal dendritic spines in a contextual fear memory engram. *Sci Rep* (2026). https://doi.org/10.1038/s41598-026-41336-2

Matthew Tennin, Hunter T. Matkins, Lindsay Rexrode, Ratna Bollavarapu, Tanya Pareek, Daniel Kroeger, Harry Pantazopoulos & Barbara Gisabella

Sleep Deprivation Alters Hippocampal Dendritic Spines in a Contextual Fear Memory Engram

Matthew Tennin[a], Hunter T. Matkins [a], Lindsay Rexrode[a], Ratna Bollavarapu[a], Tanya Pareek [a], Daniel Kroeger[c], Harry Pantazopoulos[a,b] and Barbara Gisabella[a,b]

[a]Department of Psychiatry and Human Behavior, University of Mississippi Medical Center, Jackson, MS, USA

[b]Program in Neuroscience, University of Mississippi Medical Center, Jackson, MS, USA

[c] Department of Anatomy, Physiology, and Pharmacology, College of Veterinary Medicine, Auburn University

Address for correspondence:

Barbara Gisabella, PhD

Department of Psychiatry and Human Behavior

University of Mississippi Medical School

TRC 408

2500 North State St

Jackson, MS 39232, USA

Phone: (601) 815-7984

Tennin, et al
E-mail: bgisabella@umc.edu

Abstract

Sleep is critically involved in strengthening memories. However, our understanding of the morphological changes underlying this process is still emerging. Recent studies suggest that specific subsets of dendritic spines are strengthened during sleep in specific neurons involved in recent learning. Contextual memories associated with traumatic experiences are involved in post-traumatic stress disorder (PTSD) and represent recent learning that may be strengthened during sleep. We tested the hypothesis that dendritic spines encoding contextual fear memories are selectively impacted by sleep deprivation. Furthermore, we tested how sleep deprivation after initial fear learning impacts dendritic spines following re-exposure to fear conditioning. We used ArcCreER^{T2} mice to visualize neurons that encode contextual fear learning (Arc+ neurons), and concomitantly labeled neurons that did not encode contextual fear learning (Arc- neurons). Dendritic branches of Arc+ and Arc- neurons were sampled using confocal imaging to assess spine densities using three-dimensional image analysis from either sleep deprived (SD) or control mice allowed to sleep normally. Mushroom spines in Arc+ branches displayed decreased density in SD mice. In comparison, no changes were observed in dendritic spines from Arc- branches. When animals were re-exposed to contextual fear conditioning 4 weeks later, we observed lower density of mushroom spines in both Arc+ and Arc- branches, as well as lower density of thin spines in Arc- branches in mice that were SD following the initial fear conditioning trial. Our findings indicate that sleep deprivation following exposure to contextual fear conditioning selectively impacts dendritic spines in neurons that recently encoded fear memory, both initially and following later re-exposure. SD following a

traumatic experience thus may represent a promising strategy for modifying the strength of contextual memories associated with trauma and PTSD.

Introduction

The idea that memories are strengthened or consolidated during sleep is well-established (for review see [1]). However, evidence regarding the morphological and molecular underpinnings of memory consolidation during sleep has only recently emerged. A series of studies by Tononi and Cirelli developed the synaptic homeostasis hypothesis of sleep [2,3]. This hypothesis posits that as organisms interact with their environment and encode new memories during wakefulness, neurons form new synapses and strengthen existing ones. During sleep, when the active encoding process is offline, synapses are downscaled to prevent over-excitation of neurons and improve signal-to-noise ratio and memory performance [2,3]. In support of this hypothesis, several studies have reported an overall decrease in dendritic spines, synaptic density, and synaptic markers during sleep in sensory and motor cortical regions [4-6]. However, an opposing view suggests that rather than collectively downscaling all synaptic connections, specific synapses that were recently involved in memory formation may be strengthened during sleep [7-9].

Several recent studies also suggest that the process of dendritic spine regulation during sleep is not a uniform downscaling of all synapses, but a more complex process including selective upscaling (i.e. synaptic strengthening) and downscaling (synaptic weakening) of specific dendritic spines depending on recent experiences [10-13]. For example, Born and

colleagues propose that selective synapses formed during the day are tagged by specific proteins for strengthening during sleep to reorganize memory storage [14,15]. Support for this theory comes from data demonstrating that sleep deprivation (SD) impairs memory strength [7], and results in decreased dendritic spines [8], suggesting that selective synapses may indeed be strengthened during sleep. For example, dendritic spine formation in specific branches of layer V motor cortex neurons is increased after motor learning [9], even though cortical areas may be subjected to an overall net synaptic downscaling during sleep [4,5]. Short-term (5 hours) of SD was shown to result in reduced long term plasticity in CA1 hippocampal neurons [7], and reduced dendritic spine density [8], suggesting sleep is required for synapse stabilization in this region.

What may be the cause of the discrepancies in theories regarding dendritic spine changes during sleep? One critical factor in answering this question is dissociating which neurons were recently active and engaged in learning and which were not. For example, contextual memories associated with stressful experiences such as fear are necessary for survival and represent recent learning in dendritic spines that may be strengthened during sleep. By tagging dendritic spines of neurons recently engaged in fear learning, we can separate them from others and determine how each population is modified after sleep deprivation.

To determine the impact of SD on neurons recently involved in contextual fear learning, we used ArcCreER^{T2} mice, which allowed us to permanently label fear memory engram neurons [16-19]. By concurrently labeling non-engram neurons using a viral labeling approach, we created two sets of clearly delineated neuronal populations which allowed us to assess whether dendritic spines that encode contextual fear memory are selectively modified during sleep. This is highly relevant since several recent studies suggest that SD

following emotional learning may be a promising preventative measure for post-traumatic stress disorder (PTSD) [20-22].

Furthermore, since repeated re-exposure to trauma is often a significant contributor to PTSD risk and symptom severity [23-27], we examined the effect of SD on contextual fear memory strength following a second exposure to a traumatic event. Specifically, we tested the hypothesis that SD following initial fear learning not only disrupts dendritic spine upscaling following the first exposure but may also disrupt this process following re-exposure to contextual fear conditioning 4 weeks later.

Methods

All animal procedures met National Institutes of Health standards, as outlined in the Guide for the Care and Use of Laboratory Animals, and all protocols were approved by the University of Mississippi Medical Center Institutional Animal Care and Use Committee (IACUC). Methods are reported in accordance with ARRIVE guidelines.

Animals

We used adult (3-4 months old) male ArcCreER^{T2} mice 22-25 grams in weight (Jackson Labs stock# 022357), n=4 per group for control or SD groups in our initial experiment and n=4 per group for control or SD groups in the re-exposure experiment. Animals were maintained on a 12:12 h light-dark cycle with ad libitum access to water and food. These mice express Cre-ER^{T2} under the direction of an Activity Regulated cytoskeletal associated protein (Arc) promoter region that is activated during fear-conditioned learning [17-19,28]. These mice have been well characterized for selectivity of Arc expression in the fear memory engrams [17-19,28].

Viral Vector Injection

ArcCreER^{T2}mice were anesthetized with 3% isoflurane for induction and 1.5% for maintenance. Isoflurane was administered with an induction chamber followed by a cone system during the entire procedure. The depth of anesthesia was monitored by regular testing of withdrawal reflexes (tail and paw pinch) and constant observation of respiratory rate and responses to tissue manipulation. Animals received bilateral stereotaxic microinjections of a cocktail of 2 µl of AAV mCherry ChR2 viral vector per hemisphere for a total of 4 µl/animal under the control of the CMV promoter (AAV2-CMV-DIO-mCherry), and 2 µl per hemisphere for a total of 4 µl/animal of AAV1-CMV-eGFP virus (Vector Biolabs, cat# 7002). The virus cocktail was infused using a Nanofil 35-gauge stainless steel bevel needle (catalog # NF35BV, World Precision Instruments, Inc., Sarasota, FL) attached to a 10µl Nanofil syringe (Hamilton Company, Reno, NV) as described in our previous study [29]. Hamilton syringes were mounted in a stereotaxic barrel holder, and the rate of virus delivery was controlled by an automated syringe pump (Harvard Apparatus, Holliston, MA). The injections targeted the CA1 region of the dorsal hippocampus (stereotaxic coordinates AP: -2.1, ML:1.75, DV:1.0). The AAV2 serotype was selected for the mCherry ChR2 viral vector as this serotype has been reported to result in minimal spread and shows preference for labeling neurons over other cell types [30] (Vector Labs, cat# 7104). Specifically, injections of the AAV virus under the CMV promoter allowed for the labeling of dendritic branches for spine analysis. The neurons participating in the memory trace are labeled because the contemporaneous injection of 4-OH-tamoxifen allows the CreER to enter the cell nucleus, where it may cause recombination events at loxP-flanked sites, permanently marking the cells that participated in that memory trace. Cells that are transduced with viral vectors allow for

Cre-dependent expression of ChR2-mCherry, permanently marking the cells that participated in that memory trace in red. This design allowed for visualization of neurons that are part of the fear memory engram, expressing both ChR2-mCherry from the Arc promoter (Arc+). Neurons not part of the fear memory engram (Arc-) express only GFP. After 6 weeks, animals were divided randomly into two cohorts of four mice each (4 controls, and 4 SD mice).

Contextual Fear Conditioning

Mice were given 36 days for recovery from surgery and optimal viral vector expression. Then they were placed in darkness for 12 hours to avoid non-specific Arc-YFP labeling as established by previous studies 16-19, (Fig. 1A). Mice were administered intraperitoneal injections of 4-OH-tamoxifen in the middle part of their prior dark cycle (1 AM). 4-OH-tamoxifen in mice has been established to reach detectable levels rapidly, peak between 5-9 hours following injection, and disappear almost completely by 36 hours, thus restricting stimuli via dark housing during this time window reduces non-specific YFP expression 17,28,31,32. Four hours later (5 AM), the mice underwent auditory fear conditioning to activate CreERT2 production. Fear conditioning was conducted as in our previous studies 33,34. This time point is chosen to allow fear-conditioned animals to sleep during their normal sleep period after fear learning. Briefly, mice were placed in a fear conditioning box (64cm wide ~ 73 cm deep ~ 68cm high) (Med Associates, St. Albans, VT, USA) placed in a larger, sound-attenuating chamber. Four mice were placed in 4 boxes (one mouse for each box) at the same time for experimental comparison. Mice remained in the chambers for three minutes before delivery of four tones, each of 10 seconds duration (85dB, 10kHz). Each tone was followed by a footshock lasting 2 seconds (0.8 mA amplitude) pairings were administered (60–200 s variable ITI) (total time mice spent inside

the chamber was 15-18 mins). Freezing behavior was defined as periods of at least 1 s with the complete absence of movement except breathing and was measured with manual scoring. The percent of time spent freezing during intervals of interest was quantified using VideoFreeze software (Med Associates, St. Albans, VT, USA).

Animals were either allowed to sleep normally afterwards or underwent 5 hours of SD using an automated sleep deprivation procedure (see below). Animals were then placed back into a dark environment for 48 hours following fear conditioning to avoid non-specific Arc-YFP labeling, as established by previous studies [17-19,28]. We used two experimental groups of 4 control and 4 SD animals in each group. The first group was used to examine the effect of SD on dendritic spines immediately following fear learning (Fig. 1A). The second group of mice was used to examine the effect of SD following initial fear learning on dendritic spines after re-exposure to the fearful stimulus 4 weeks later (Fig. 1B). Our experimental timelines were guided by similar procedures reported in prior studies using ArcCreER^{T2} (Cazzulino et al. 2016)

Automated Sleep Deprivation

The Pinnacle automated sleep deprivation system (Cat# 9000-K5-S) which simulates gentle handling was used for 5 hours of sleep deprivation from lights on (6 AM) to 11 AM. This system consists of a cylindrical housing chamber with a bar that continuously rotates at 5 rpm and randomly reverses direction every 10–30 s, which prevents animals from sleeping. All animals were housed in the cylindrical chambers beforehand to adapt to the environment and control animals were housed in the same chambers but without the rotating bar. A researcher visually verified that the bar always rotated and that mice did not use alternative strategies to avoid the bar and sleep. This system has been established

by prior studies to effectively reduce sleep as measured with EEG recordings in rats and mice [29,35-38]. Both control and SD mice were sacrificed at 11 AM and processed for quantification of dendritic spines (Fig. 1). This time point (5 h into the light cycle) is identical to previous studies from our lab and others [29,39,40]. Brains were then analyzed for viral vector expression and dendritic spine density as in our published studies [29,39].

Tissue processing

Mice were sacrificed by cervical dislocation and perfused with 0.1M phosphate-buffered saline (PBS) containing 4% paraformaldehyde. Brains were removed and cryoprotected in 30% sucrose in 0.1M PBS (pH 7.4), then sectioned into coronal 40 µm serial sections using a freezing microtome (American Optical 860, Buffalo, NY) and stored in 0.1M phosphate buffer with 0.1% NaAzide. Sections were mounted on gelatin-coated slides and coverslipped using Dako mounting media (S3023, Dako, North America, Carpinteria, CA) to quantify dendritic spine density from images captured using confocal microscopy.

Confocal imaging

A Zeiss LSM 880 confocal microscope system interfaced with Zen imaging software (ZEN 2.3 SP1) was used to acquire 3D image stacks of dendritic branches from hippocampal CA1 neurons in sections from control and SD mice. All slides used for confocal imaging were coded for blind analysis and experimenters were blinded to the definition of green vs red labeling in order to avoid bias. Images of 40 µm-thick sections were acquired, with a z-step of 0.5 µm using a 63x oil immersion objective (numerical aperture 1.4 DIC M27; pixel size, 0.10 x 0.10 µm) similar to the method described in our previous study [29,33]. For dendritic spine quantification, confocal microscopy images were analyzed using Neurolucida 360 software with Autospine to measure spine density in hippocampus CA1

cells using an approach previously described [33,39,41,42]. Dendritic spines were sampled in the CA1 area of the hippocampus by an investigator who was blinded to the treatment group. We collected confocal images of all visible viral vector-labeled dendritic branches in stratum radiatum (apical dendrites) within the CA1 area of the hippocampus using 25x25 µm confocal imaging windows. Analysis was restricted to stratum radiatum, as this was the area where the majority of Arc+ dendrites were observed. Slides were coded for blind analysis, and sampling boxes were placed in the CA1 area. The length from the border of CA2 to the medial end of CA1 was measured for each section, and sampling boxes were placed on either side of the mid-point between these two ends of CA, halfway between the lateral border of CA1/CA2 and the medial end of CA1. Two sampling boxes (450×300 µm^2) were placed in the stratum radiatum each 300 µm left and right of the midline, positioned immediately below the pyramidal cell layer. Sampling boxes were placed within the injection site radius beginning at a distance sufficiently away from the primary site of injection to allow for reliable identification of individual dendritic branches while ensuring that sampling sites were still within the viral injection site zone. This approach also ensured that both red and green spines were sampled in the same sampling sites from the same injection zone in order to prevent sampling bias. Due to the density of fluorescently labeled dendritic branches within the injection site zone, it was not feasible to distinguish branch order of the sampled branches. We then imaged all dendrites located in each box visible with Arc+ (Chr2-mCherry red), or Arc- (YFP green) fluorescence.

Dendritic spine quantification

For dendritic spine quantification, confocal microscopy images were analyzed using Neurolucida 360 software with Autospine to measure spine density as described in our previous study [29,33,39]. Spines were grouped into thin spines, stubby spines, and mushroom

spines automatically by the Neurolucida 360 software based on the spine head to neck diameter ratio (1.1), length-to-head ratio (2.5) mushroom head size (0.35 μm), and filopodia length (3 μm) according to previously established criteria [42]. Spine density, shape, and volume were quantified using Neurolucida 360 with semiautomated analysis from 3D confocal image stacks in an unbiased manner. Experimenters were blinded to the definition of green vs red labeling in order to avoid bias.

Statistical analysis

Densities of dendritic spines were calculated as spines per dendrite segment length in micrometers. For all statistical tests, the significance threshold was $p \leq 0.05$ followed by Bonferroni post hoc correction. Non-parametric (Wilcoxon-Mann-Whitney) tests were used to compare population estimates for control and SD groups as data were not normally distributed and were followed by Bonferroni post hoc correction. Box plots were used to depict the data for each group from n= 4 control and n= 4 SD animals).

RESULTS

Sleep deprivation following fear learning decreases dendritic spines in the contextual fear memory engram.

Significance values for all dendritic spine measures were calculated using non-parametric (Wilcoxon-Mann-Whitney) tests followed by Bonferroni post hoc correction and reported as p-values, F-ratios, t-ratios, and Z-values where statistical significance was detected. Arc+ branches were largely distributed in stratum radiatum of CA1 (Fig 2A), and dendritic spine densities were quantified from Arc+ and Arc- branches (Fig. 2B,C). No significant difference was observed in overall spine density between SD and control mice (Fig. 2 D). We observed significantly lower density of mushroom spines in SD mice compared to

control mice (p□0.004, F-ratio: 9.92, t-ratio: -3.15, Z-value: -2.93, Fig. 2E). Overall densities of thin and stubby spines did not differ between SD and control animals (Fig. 2E). Decreased densities of mushroom spines were observed in Arc+ branches of SD mice, indicating that the differences in mushroom spines in SD animals were driven by neurons that encoded the recent contextual fear memory (p□0.001, F-ratio: 18.29, t-ratio: -4.28, Z-value: -3.86, Fig. 2G). In comparison, densities of stubby spines were increased in Arc+ branches of SD mice in comparison to controls (p□0.05, F-ratio: 10.53, t-ratio: 3.25, Z-value: 2.03, Fig. 2G) which did not achieve significance after multiple comparison correction. No changes in dendritic spine densities from Arc- branches were detected between SD and control animals (Fig. 2H,I).

Sleep deprivation following fear learning alters dendritic spine head and neck length

Dendritic spine neck length is associated with the rate of synaptic transmission and synaptic strength, with shorter length associated with faster synaptic transmission [43]. Significantly shorter spine head and neck length was observed specifically for thin spines (head length: p□0.002; F-ratio: 11.38, t-ratio: -3.37, Z-value: -3.79, Fig. 3A) and neck length: (p□0.001; F-ratio: 12.17, t-ratio: -3.49, Z-value: -4.12, Fig. 3B) from Arc+ branches in SD mice compared to control mice. No changes in spine head length were detected in mushroom and stubby spines in Arc+ branches (Fig. 3A,B). In comparison, Arc- branches displayed significantly shorter spine head length in mushroom spines (head length: F-ratio: 0.39, t-ratio: -0.62, Z-value: -2.00, p□0.05) and stubby spines (p□0.02; F-ratio: 5.72, t-ratio: -2.39, Z-value: -2.29, Fig. 3C) which did not achieve significance after multiple comparison correction, along with greater head length of thin spines (p□0.005; F-ratio: 12.07, t-ratio: 3.47, Z-value: 2.84, Fig. 3C) in SD mice compared to control mice. Neck backbone length

in spines from Arc- branches was increased in thin spines ($p<0.01$; F-ratio: 10.68, t-ratio: 3.27, Z-value: 2.55, Fig. 3D) and decreased in stubby spines ($p<0.001$; F-ratio: 5.94, t-ratio: -2.44, Z-value: -4.06, Fig. 3D) from SD mice compared to control mice.

Sleep deprivation after fear learning alters dendritic spine head and neck diameter, volume, and surface area

Dendritic spine neck diameter is normally positively correlated with head volume [44,45]. No changes in overall spine head and neck diameter were detected in thin, mushroom, or stubby spines of Arc+ branches in SD mice compared with control mice after fear conditioning (Fig. 4A-B). In contrast, Arc- branches from SD mice displayed greater head and neck diameter specifically in stubby spines (head diameter: $p<0.001$; F-ratio: 20.43, t-ratio: 4.52, Z-value: 4.38, Fig. 4C; neck diameter: $p<0.001$; F-ratio: 20.66, t-ratio: 4.55, Z-value: 4.47, Fig. 4D). Spine volume and surface area is a measure of synaptic strength and is positively associated with the density of glutamate receptors [46-49]. Smaller spine surface area and volume in Arc+ branches was observed in thin spines from SD mice versus control mice (volume: $p<0.03$; F-ratio: 18.70, t-ratio: -4.33, Z-value: -2.17, Fig. 4E; surface area: $p<0.03$; F-ratio: 18.47, t-ratio: -4.30, Z-value: -2.20, Fig. 4F) which did not achieve significance after multiple comparison correction. Moreover, we observed greater surface and volume for stubby spines in Arc- branches (volume : $p<0.03$; F-ratio: 2.30, t-ratio: 1.52, Z-value: 2.56; Fig. 4G) which did not achieve significance after multiple comparison correction, and surface area: ($p<0.01$; F-ratio: 2.81, t-ratio: 1.68, Z-value: 2.56, Fig. 4H).

Sleep deprivation following initial fear learning impacts dendritic spine measures after re-exposure to contextual fear conditioning 28 days later

We tested the hypothesis that SD after the initial fear conditioning session impacts

synaptic changes that occur following future re-exposure to the traumatic experience by re-exposing mice to fear conditioning 28 days later. Spine density across all spines (Arc+ and Arc- combined) was significantly decreased in SD mice compared with control mice after fear conditioning re-exposure ($p<0.001$; F-ratio: 35.94, t-ratio: -5.99, Z-value: -4.77, Fig. 5A). This decrease was selective for thin spines ($p<0.007$; F-ratio: 21.78, t-ratio: -4.67, Z-value: -3.40, Fig. 5B). Mice that were sleep disrupted following the initial fear conditioning session displayed a trend towards lower freezing during re-exposure 28 days later, with significantly lower freezing duration during the first post-tone interval and increasing to control levels by the 3rd post-tone interval (Fig. 5C). Moderate effects were observed in dendritic spine densities from Arc+ branches. No change was observed in overall density of Arc+ spines (Fig. 5D), possibly due to opposite changes in mushroom vs thin spines. Mushroom spine density was significantly decreased in SD mice compared to control mice ($p<0.001$; F-ratio: 2.94, t-ratio: -1.71, Z-value: -3.15, Fig. 5E), whereas thin spine density was increased in SD mice ($p<0.002$; F-ratio: 25.73, t-ratio: 5.07, Z-value: 6.44, Fig. 5E). In comparison, Arc- branches displayed an overall decrease of dendritic spine density in SD mice ($p<0.001$; F-ratio: 39.17, t-ratio: -6.26, Z-value: -5.07, Fig. 5F), that was significant for thin ($p<0.001$; F-ratio: 71.94, t-ratio: -8.48, Z-value: -7.53, Fig. 5G) and mushroom spines ($p<0.003$; F-ratio: 13.37, t-ratio: -3.66, Z-value: -2.99, Fig. 5G). Stubby spines from Arc- branches displayed significantly greater density in SD mice ($p<0.02$; F-ratio: 19.38, t-ratio: 4.40, Z-value: 2.53, Fig. 5G) which did not achieve significance after multiple comparison correction. Furthermore, significant positive correlations were observed between densities of Arc+ thin spines and post-tone 1 (PT1) freezing levels in control and SD animals (Fig. 5H&J). No significant correlations were detected for Arc- thin spine densities with PT1 freezing levels (Fig. 5I&K).

Sleep deprivation following initial fear learning alters dendritic spine head and neck length

after re-exposure to fear conditioning 28 days later

Thin spines from Arc+ branches from SD mice displayed significantly shorter head and neck length compared to control mice head length: ($p<0.001$; F-ratio: 17.74, t-ratio: -4.21, Z-value: -6.28, Fig. 6A) and neck length: ($p<0.001$; F-ratio: 53.22, t-ratio: -7.30, Z-value: -10.25, Fig. 6B) following re-exposure to fear conditioning. Greater neck length was observed for mushroom spines from Arc+ branches in SD mice compared to control mice neck length: ($p<0.04$; F-ratio: 0.68, t-ratio: 0.26, Z-value: 2.08, Fig. 6B) that did not attain significance after correction for multiple comparisons. No difference was observed for head or neck length in stubby spines from Arc+ branches between SD and control mice (Fig. 6A,B). In comparison Arc- branches of SD mice displayed greater head and neck length of thin spines head length: ($p<0.001$, F-ratio: 122.84, t-ratio: 11.08, Z-value: 11.67); neck length: ($p<0.001$, F-ratio: 106.66, t-ratio: 10.33, Z-value: 10.38), (Fig. 6C-D) and greater head length for mushroom spines ($p<0.01$, F-ratio: 15.97, t-ratio: 3.99, Z-value: 2.67). Shorter head and neck length was observed for stubby spines from Arc- branches of SD mice compared to control mice head length: ($p<0.004$, F-ratio: 4.31, t-ratio: -2.08, Z-value: -2.95); and neck length ($p<0.001$; F-ratio: 23.68, t-ratio: -4.87, Z-value: -5.54, Fig. 6C-D).

Sleep deprivation following initial fear learning alters dendritic spine head and neck diameter and spine size after re-exposure to fear conditioning 28 days later

Smaller head diameter was observed for mushroom spines from Arc+ branches from SD mice compared to control mice ($p<0.006$; F-ratio: 17.45, t-ratio: -4.18, Z-value: -2.77, Fig. 7A), along with greater head and neck diameter of thin spines: head diameter: ($p<0.001$;

F-ratio: 190.78, t-ratio: 13.81, Z-value: 16.86, Fig. 7A); neck diameter: ($p<0.001$; F-ratio: 167.84, t-ratio: 12.95, Z-value: 15.55, Fig. 7B). In comparison, greater head diameter was observed in mushroom spines from Arc- branches that did not achieve significance after correction for multiple comparisons head diameter: ($p<0.04$; F-ratio: 4.19, t-ratio: 2.05, Z-value: 2.07, Fig. 7C), along with greater head and neck diameter of stubby spines: head diameter: ($p<0.001$; F-ratio: 20.96, t-ratio: 4.58, Z-value: 5.94, Fig 7C); neck diameter: ($p<0.001$; F-ratio: 21.15, t-ratio: 4.60, Z-value: 5.91, Fig. 7D) in SD vs control mice. Thin spines from Arc- branches displayed smaller neck diameter in SD mice: neck diameter: ($p<0.001$; F-ratio: 5.69, t-ratio: -2.39, Z-value: -2.69, Fig. 7D). Smaller volume of mushroom spines was detected in Arc+ branches from SD mice ($p<0.001$; F-ratio: 59.50, t-ratio: -7.71, Z-value: -4.42, Fig. 7E), along with smaller volume and surface area of stubby spines (volume: $p<0.001$; F-ratio: 127.52, t-ratio: -11.29, Z-value: -11.93, surface area: $p<0.001$; F-ratio: 138.56, t-ratio: -11.77, Z-value: -10.83, Fig. 7E&F). Increased volume and surface area were detected for all spine types from Arc- branches from SD mice compared to control mice: mushroom volume: ($p<0.001$; F-ratio: 26.80, t-ratio: 5.18, Z-value: 4.39, Fig. 7G); mushroom surface area: ($p<0.001$; F-ratio: 38.60, t-ratio: 6.21, Z-value: 5.26, Fig. 7H); stubby volume: ($p<0.001$; F-ratio: 118.67, t-ratio: 10.89, Z-value: 16.436, Fig. 7G); stubby surface area: ($p<0.001$; F-ratio: 178.34, t-ratio: 13.35, Z-value: 15.48, Fig. 7H); thin volume: ($p<0.001$; F-ratio: 89.10, t-ratio: 9.44, Z-value: -10.48, Fig. 7G); thin surface area: ($p<0.001$; F-ratio: 114.27, t-ratio: 10.69, Z-value: 10.85, Fig. 7H).

DISCUSSION

Our results demonstrate that SD following contextual fear learning alters dendritic spines in the fear memory engram of CA1 neurons compared to mice without SD following contextual fear learning (Fig. 8). This represents, to our knowledge, the first evidence for

morphological synaptic alterations in SD mice in a hippocampal fear memory engram and provides key insight regarding reports of synaptic upscaling vs synaptic downscaling in this region during sleep [8,39,50]. Our observed impact of SD on dendritic spine morphology and density may reflect several possibilities including impairment of active strengthening of Arc+ spines during sleep, impaired maintenance of learning-induced changes in Arc+ spines, or an impact on global synaptic downscaling during sleep in which Arc+ synapses were relatively protected.

Furthermore, our findings suggest that re-exposure to contextual fear conditioning results in dendritic spine alterations in neurons that were not part of the original contextual memory engram, thus expanding the engram, and that SD after initial fear learning impairs this process that occurs following re-exposure (Fig. 5). Furthermore, mice that were sleep disrupted following the initial fear conditioning session displayed a trend towards less freezing during re-exposure to fear conditioning 28 days later (Fig. 5). Together our results provide insight into the contextual fear engram specific morphological alterations that occur during sleep and support the potential therapeutic and protective effect of SD following a traumatic experience.

Although our we cannot rule out other possibilities, one possibility is that our observed findings may reflect upscaling and downscaling processes that occur during sleep. Previous studies, including from our group, reported broad downscaling of dendritic spines in CA1 during sleep [39,50], opposite to our current findings of selective upscaling of dendritic spines following fear learning. The broad downscaling in our previous study occurred in mice without recent learning [39], and the study in adolescent mice was conducted following exposure to novel objects [50], which does not represent the biologically relevant emotional

learning that occurs during fear conditioning. Broad downscaling during sleep thus may be a standard process to enhance signal to noise ratio following standard contextual encounters, whereas recent emotional learning from that occurs during stressful experiences that may be necessary for survival results in selective upscaling during sleep in the same hippocampal region.

Recent evidence demonstrated that sleep following contextual fear conditioning in mice suppressed cFos and Arc protein expression in the CA1 region compared to mice that underwent 6 hours of SD [51]. Furthermore, sleep following contextual fear conditioning also suppressed phosphorylated S6 and ERK1/2 compared to mice that underwent SD, along with CA1 specific transcriptional alterations [51]. Phosphorylated S6 and ERK1/2 are increased by neuronal activity and involved in promoting formation and maintenance of dendritic spines [52-55], suggesting these molecular processes and the reported associated transcriptional pathways may underlie our observed dendritic spine changes in Arc+ neurons following contextual fear learning.

The majority of Arc+ dendrites observed in CA1 were located in the stratum radiatum (Fig. 2A). The CA1 stratum radiatum has been implicated as a key site of contextual fear memory consolidation [56], and is the CA1 layer where dendritic spine potentiation following contextual fear conditioning recall was reported to occur [57]. Apical dendrites of CA1 pyramidal neurons receive synaptic inputs from CA3 Schaffer collaterals onto mid and proximal apical segments [58], and are involved in the formation of emotional memory [59,60]. Apical dendrites in CA1 contextual fear memory engram cells display increased density and size of dendritic spines receiving inputs from CA3 contextual fear memory engram cells following contextual fear learning [61]. Our evidence for synaptic upscaling during sleep

in Arc+ branches, including greater densities of mushroom spines and enhanced spine morphology (Fig. 2,4) suggests that connections from CA3 to CA1 following fear learning are strengthened during sleep. The spine morphology changes we observed, indicating enhanced memory storage during sleep in Arc+ spines immediately after fear learning, is in line with reports that spine morphology is enhanced in fear memory engram cells and prior studies suggest this correlates with fear memory strength [62]. Furthermore, our findings indicate that SD after initial fear learning impairs strengthening of dendritic spines that occurs in engram cells as well as enlargement of the engram following re-exposure 28 days later (Fig. 5). Thus, SD after the initial fear learning may alter morphological and molecular processes that impact CA3 to CA1 connections that guide short and long-term memory consolidation and reconsolidation processes.

The volume and surface area of Arc+ thin spines was increased during sleep following initial fear learning, compared to the SD animals (Fig. 4). Greater surface area and volume indicate synaptic upscaling during sleep following contextual fear conditioning, as greater spine volume and surface area is associated with synaptic strength and density of glutamate receptors [46-49]. Taken together with increased density of mushroom spines in Arc+ branches, this suggests that thin spines that participated in encoding contextual fear memory are in the process of synaptic enhancement during sleep and may develop into mushroom spines [63]. Previous studies have demonstrated that increased synaptic plasticity is associated with a morphological shift from thin to mushroom spines [64-67]. Arc- neurons in contrast did not display altered spine densities. Furthermore, the morphological changes observed including increased head and neck length of mushroom spines and stubby spines (Fig. 3), and decreased head and neck diameter, volume, and surface area of stubby spines (Fig. 4) in control mice compared to SD mice, indicate weaker

strength of spines that are not involved in encoding contextual fear memory in animals that sleep normally compared with SD animals following contextual fear conditioning.

In comparison, fear re-exposure resulted in shorter neck length of mushroom spines in Arc+ branches during sleep (Fig. 6), which is associated with faster synaptic transmission and greater synaptic strength [43]. Furthermore, mushroom spines in Arc+ branches displayed greater head diameter and volume during sleep (Fig. 7), indicating morphological strengthening of mushroom spines during sleep following fear re-exposure in the original contextual fear engram. Arc- branches displayed shorter head and neck length of thin and mushroom spines, along with smaller volume and surface area of all spine types during sleep following re-exposure (Fig. 7). When taken together with increased density during sleep in Arc-branches (Fig. 5), this suggests more moderate morphological changes during sleep as neurons that were not part of the original contextual fear memory trace are recruited into this trace following re-exposure. Overall, these findings suggest that sleep after re-exposure to a traumatic experience strengthens the contextual fear memory trace during sleep both in neurons that originally encoded this memory as well as neurons that were not part of the original memory engram, indicating expansion of the engram.

Our findings suggest that sleep after a traumatic experience strengthens dendritic spines in the contextual fear memory engram. Our data, together with previous studies demonstrate that SD following fear conditioning impairs contextual fear memory [68,69], including work from our group [34], which suggests that SD after a traumatic experience may alleviate PTSD risk by preventing the strengthening of dendritic spines that encode

contextual fear memory. Evidence that sleep deprivation reduces emotional memories in human subjects [21] provides further support for this protective effect.

Multiple traumatic experiences increase the risk of developing PTSD as well as the severity of PTSD symptoms [23-27]. Therefore, we tested the hypothesis that SD following the initial traumatic event (initial fear conditioning session) alters dendritic spines in the contextual fear memory engram following re-exposure to the traumatic event 28 days later. Our findings demonstrate that in control mice, re-exposure to fear conditioning results in greater synaptic strength in the original contextual fear memory engram neurons as well as in neurons that were not part of the original engram, suggesting expansion of the contextual fear memory engram following re-exposure. Synaptic strengthening in neurons that were not part of the original memory trace may contribute to generalized contextual fear inherent in PTSD [70,71]. Furthermore, SD following the initial fear conditioning session resulted in significantly decreased synaptic measures that are associated with stronger synapses compared with control animals following re-exposure, particularly in neurons that were not part of the original engram and weakened freezing during re-exposure (Fig. 5). This suggests that SD following a traumatic experience may be a protective factor for potential re-exposure to a traumatic event and possibly alleviate PTSD risk and severity. The observed significant positive correlations of densities of Arc+ thin spines but not Arc- thin spines with post-tone 1 freezing levels supports this hypothesis (Fig.5H-K). Evidence that sleep after learning enhances emotional memories in humans for up to 4 years [72], provides support for such long-term protective effects of SD following emotional learning.

It is important to note that our observed effects of SD on synaptic properties may be due to the general effects of sleep deprivation itself rather than an effect of SD impacting the

fear learning process. While we discuss synaptic upscaling and downscaling as a possible interpretation, this reflects one of several possibilities mentioned above. Future studies developing approaches to allow for comparison of our findings with similar measures in animals without contextual fear conditioning with and without SD, and/or real time in vivo measures of dendritic spines will clarify these possibilities. Our statistical analysis compared measures of all dendritic branches for spine densities and measures of all spines for morphological measures regardless of which animal they were sampled from, as conducted in several previous studies of dendritic spines including from our group [11,29,39,47,73-75]. However, due to our sampling strategy in which we captured and quantified all viable dendritic branches in our sampling fields for each animal, this resulted in a high degree of variability in the numbers of sampled branches between animals as seen in the bee swarm plots. Future studies designed employ equal sampling in terms of number of dendrites and spines per animal will provide further information regarding the variability of these findings between animals. The lack of dendritic branch and segment specific analysis in our study is an important limitation. The limited distribution of Arc+ and Arc- neurons and their dendritic branches in CA1 concentrated in the virus injection site made it challenging to follow branches from individual neurons. However, obtaining information regarding dendritic spines measures from neurons that were part of the contextual fear memory engram vs neurons that were not in SD and control animals for 3-dimensional high resolution dendritic spine quantification was important. Therefore, we analyzed all clearly visible Arc+ and Arc- labeled dendritic branches in our samples. Lack of cell type specificity for the dendritic spines sampled is another potential limiting factor in understanding how dendritic spines may be altered during sleep in specific populations of excitatory and inhibitory neurons. Arc is only expressed in excitatory neurons [76], thus our design using ArcCreER^{T2} mice allowed for selective analysis of dendritic spines in

excitatory neurons. Selective changes in somatostatin inhibitory neuron populations for example have been reported recently in CA1 following 6 hours of sleep deprivation [77]. Future studies designed to examine dendritic spines in inhibitory neurons may reveal differential dendritic spine changes during sleep in inhibitory neuron populations, as suggested by recent evidence for a key role of hippocampal somatostatin neurons during sleep [78]. ArcCreER^{T2} mice mice have been well characterized for selectivity of Arc expression in the fear memory engrams [17-19,28]. The Arc protein is localized to dendritic spines, particularly in sites of increased postsynaptic activity [79]. Importantly, extensive evidence supports the role of Arc in memory formation and consolidation (for review see [79] and [80]). However, hippocampal region-specific molecular alterations have been reported in SD mice following contextual fear conditioning [51]. This suggests dendritic spine changes may vary by region, particularly during re-exposure to fear conditioning 28 days after the initial learning. Future studies will examine engram specific dendritic spine changes in SD mice from other hippocampal sectors and the overlap of re-activation of the original Arc labelled neurons at later timepoints.

Conclusion

In summary, our findings represent the first evidence for contextual fear memory engram dendritic spine changes in the hippocampus following SD. Collectively, our data indicate that SD alters dendritic spines in the contextual fear memory engram. Furthermore, our findings suggest that later re-exposure to contextual fear conditioning expands the fear memory engram and indicate that SD following initial contextual fear learning impairs synaptic strengthening during sleep that occurs following future re-exposure to a traumatic experience.

Data Availability

The data and original contributions presented in this study are included in the manuscript and are available upon request to the corresponding author.

Acknowledgments:

This work was funded by support from NIMH R21MH117460 and NIGMS P20GM144041.

Conflict of Interest Statement: The authors have no competing financial interests to disclose.

Figure Legends:

Figure 1. Experimental timeline. Sleep Deprivation and Dendritic Spine Analysis After Initial Fear Learning: ArcCreER^{T2} mice were stereotaxically injected with dual AAV viral vectors to label dendritic spines involved in contextual fear learning (mCherry, Arc positive, Arc+) and spines not involved in contextual fear learning (eGFP, Arc negative, Arc-). (A) After 36 days, mice were placed in darkness for 12 hours to avoid any non-specific Arc induction, injected with 4-OH-tamoxifen at 1 AM, and 4 hours later underwent contextual fear conditioning, followed by 5 hours of sleep deprivation or normal sleep. Animals were then placed back into a dark environment for 48 hours and euthanized for brain sample processing. (B) Dendritic Spine Analysis After Contextual Fear Re-exposure: In the second set of experiments, animals underwent a similar timeline of procedures to label dendritic spines followed by fear conditioning with or without SD. These animals were then returned to standard housing for 4 weeks before undergoing re-exposure to contextual fear conditioning. Mice were allowed to sleep for 5 hours and were then

sacrificed for brain sample processing. Images in 1A and 1B Created in BioRender. Gisabella, B. (2025) https://BioRender.com/wd2sdvs.

Figure 2. Sleep deprivation following initial fear learning decreases dendritic spines in the contextual fear memory engram.

The majority of Arc+ branches in CA1 were distributed in stratum oriens (A), scale bar = 100 µm. Confocal images depicting representative branches and spines from Arc- (B) and Arc+ (C) neurons in CA1. Scale bars = 1 µm. No difference was observed in overall spine density between control and SD mice (D). When comparing overall spine densities for specific spine classes, there was significantly lower density of mushroom spines in SD mice (n_{mice} = 4; $n_{dendrites}$ = 223) compared to control mice (n_{mice} = 4; $n_{dendrites}$ = 260) indicating stronger synaptic strength in animals with normal sleep (E). No differences were detected for densities of thin or stubby spines. No difference in overall Arc+ spine density was detected between SD and control mice (F). Arc+ branches displayed decreased density of mushroom spines in SD mice (n_{mice} = 4; $n_{dendrites}$ = 135) compared to control mice (n_{mice} = 4; $n_{dendrites}$ = 110), indicating greater strength oof mushroom spines in animals with normal sleep in the recently encoded contextual fear memory engram. In contrast, we observed an increase in stubby spine density in Arc+ branches, and no changes were observed in thin spines (G). In comparison, Arc- branches displayed no differences in dendritic spine density (SD: n_{mice} = 4; $n_{dendrites}$ = 88; control: n_{mice} = 4; $n_{dendrites}$ = 114)(H-I). Bee swarm plots depict values for each group and colored dots represent individual values from each animal. Statistical significance was determined using the Wilcoxon-Mann-Whitney test followed by Bonferroni post hoc correction. SO: Stratum Oriens, SP: Stratum Pyramidale, SR: Stratum Radiatum.

Figure 3. Sleep deprivation following fear learning alters dendritic spine head and neck length.

The diagram depicts neck backbone length measured as the distance from the insertion point to the center of the spine head minus the head radius and anchor radius. Head backbone length is measured as the distance from the insertion point to the center of the spine head minus the anchor radius. (A,B) Significantly shorter head and neck length of thin spines was observed in Arc+ branches from SD mice compared to control mice (control; n_{mice} = 4; n_{spines} = 2289; SD; n_{mice} = 4; n_{spines} = 2063). No differences were observed in Arc+ branches for head and neck length of mushroom (control; n_{mice} = 4; n_{spines} = 1938; SD; n_{mice} = 4; n_{spines} = 2966) or stubby spines (control; n_{mice} = 4; n_{spines} = 818; SD; n_{mice} = 4; n_{spines} = 1444). Arc- branches displayed significantly shorter spine head length in mushroom spines (control; n_{mice} = 4; n_{spines} = 2717; SD; n_{mice} = 4; n_{spines} = 2055) and stubby spines (control; n_{mice} = 4; n_{spines} = 759; SD; n_{mice} = 4; n_{spines} = 661) in SD vs control mice (C,D). Greater head length of thin spines was also observed in Arc- branches of SD mice (C) spines (control; n_{mice} = 4; n_{spines} = 1563; SD; n_{mice} = 4; n_{spines} = 1061). Bee swarm plots depict values for each group and colored dots represent individual values from each animal. Statistical significance was determined using the Wilcoxon-Mann-Whitney test followed by Bonferroni post hoc correction.

Figure 4. Sleep deprivation after fear learning alters spine head and neck diameter, volume and surface area

No changes in head and neck diameter were detected in mushroom spines (control; n_{mice} = 4; n_{spines} = 1938; SD; n_{mice} = 4; n_{spines} = 2966), stubby spines (control; n_{mice} = 4; n_{spines} = 818; SD; n_{mice} = 4; n_{spines} = 1444), or thin spines (control; n_{mice} = 4; n_{spines} = 2289; SD; n_{mice} = 4; n_{spines} = 2063) spines from Arc+ branches in SD mice comparted to control mice (A).

Arc- branches displayed greater head and neck diameter of stubby spines in SD mice compared to control mice (control; n_{mice} = 4; n_{spines} = 759; SD; n_{mice} = 4; n_{spines} = 661), (C,D). Smaller volume and surface area was observed in thin spines from Arc+ branches in SD mice compared to control mice (control; n_{mice} = 4; n_{spines} = 1563; SD; n_{mice} = 4; n_{spines} = 1061), (E,F). Greater surface area and volume was observed for stubby spines from Arc- branches in SD mice compared to control mice (E,F). Bee swarm plots depict values for each group and colored dots represent individual values from each animal. Statistical significance was determined using the Wilcoxon-Mann-Whitney test followed by Bonferroni post hoc correction.

Figure 5. Sleep deprivation following initial fear learning impacts dendritic spine changes that occur after re-exposure 28 days later.

The overall spine density across both Arc+ and Arc- spines was significantly lower in SD mice (n_{mice} = 4; $n_{dendrites}$ = 768) versus control mice (n_{mice} = 4; $n_{dendrites}$ = 1245) following re-exposure to fear conditioning 28 days after the initial exposure (A). This decrease was selective for thin spines (B). Mice that were sleep disrupted following initial exposure to fear conditioning displayed a trend towards less freezing during re-exposure, with significantly lower freezing during the first post-tone (PT) interval (C). No difference was observed in overall spine density from Arc+ branches (D). Mushroom spine density was significantly lower in Arc+ branches from SD mice (n_{mice} = 4; $n_{dendrites}$ = 484) compared to control mice compared to control mice (n_{mice} = 4; $n_{dendrites}$ = 452) (E). Thin spine density was increased in SD mice compared to control mice (E). Arc- branches displayed overall lower dendritic spine density in SD mice (n_{mice} = 4; $n_{dendrites}$ = 284), compared to control mice (n_{mice} = 4; $n_{dendrites}$ = 571)(F). Lower density was present in thin and mushroom spines (G). Stubby spines from Arc- branches displayed significantly greater density in SD

mice (G). Significant positive correlations were observed between Day 28 post-tone 1 (PT1) freezing levels with densities of Arc+ thin spines but not Arc- thin spines in both control and SD animals (H-K). Bee swarm plots depict values for each group and colored dots represent individual values from each animal. Statistical significance was determined using the Wilcoxon-Mann-Whitney test followed by Bonferroni post hoc correction. Plots for fear conditioning data represent means and 95% confidence intervals and significance was determined using ANOVA for individual time points and repeated measures ANOVA across all timepoints.

Figure 6. Sleep deprivation following initial fear learning alters dendritic spine head and neck length after re-exposure to fear conditioning.

Thin spines from Arc+ branches from SD mice displayed significantly shorter head and neck length compared to control mice (control; n_{mice} = 4; n_{spines} = 2654; SD; n_{mice} = 4; n_{spines} = 2403) following re-exposure to fear conditioning (A,B). Greater neck length was observed for mushroom spines from Arc+ branches in SD mice compared to control mice (control; n_{mice} = 4; n_{spines} = 12375; SD; n_{mice} = 4; n_{spines} = 7894), (B). No difference in head and neck length was observed in stubby spines from SD mice compared to control mice (control; n_{mice} = 4; n_{spines} = 2106; SD; n_{mice} = 4; n_{spines} = 901), (A,B). Arc- branches displayed greater head and neck length of thin spines (control; n_{mice} = 4; n_{spines} = 10642; SD; n_{mice} = 4; n_{spines} = 3871) and head length of mushroom spines (control; n_{mice} = 4; n_{spines} = 9129; SD; n_{mice} = 4; n_{spines} = 4208) in SD mice compared to control mice (C,D). Shorter head and neck length was observed for stubby spines from Arc- branches of SD mice compared to control mice (control; n_{mice} = 4; n_{spines} = 1540; SD; n_{mice} = 4; n_{spines} = 957), (C,D). Bee swarm plots depict values for each group and colored dots represent individual values from each animal. Statistical significance was determined using the Wilcoxon-Mann-Whitney test followed by Bonferroni post hoc correction.

Figure 7. Sleep deprivation following initial fear learning alters dendritic spine head and neck diameter and spine size after re-exposure to fear conditioning. Smaller head diameter was observed for mushroom spines from Arc+ branches from SD mice compared to control mice (control; n_{mice} = 4; n_{spines} = 12375; SD; n_{mice} = 4; n_{spines} = 7894) following re-exposure to fear conditioning 28 days after initial exposure (A). Greater head and neck diameter of thin spines was observed in Arc+ branches from SD mice compared to control mice (control; n_{mice} = 4; n_{spines} = 2654; SD; n_{mice} = 4; n_{spines} = 2403), (A,B). Arc- branches displayed greater head diameter of mushroom spines (control; n_{mice} = 4; n_{spines} = 9129; SD; n_{mice} = 4; n_{spines} = 4208) and greater head and neck diameter of stubby spines (control; n_{mice} = 4; n_{spines} = 1540; SD; n_{mice} = 4; n_{spines} = 957) in SD mice compared with control mice (C,D). Thin spines from Arc- branches displayed smaller neck diameter in SD mice compared with control (control; n_{mice} = 4; n_{spines} = 10642; SD; n_{mice} = 4; n_{spines} = 3871), (D). Smaller volume of mushroom spines was detected in Arc+ branches from SD mice compared with control mice, along with smaller volume and surface area of stubby spines (E,F). Increased volume and surface area were detected for thin, mushroom and stubby spines from Arc- branches from SD mice compared to control mice (G,H). Bee swarm plots depict values for each group and colored dots represent individual values from each animal. Statistical significance was determined using the Wilcoxon-Mann-Whitney test followed by Bonferroni post hoc correction.

Figure 8. Summary of Dendritic Spine Changes During Sleep in the CA1 Contextual Fear Memory Engram. The diagram represents a summary of the working hypothesis of dendritic spine changes during sleep in CA1 neurons that initially encoded fear memory (Arc+) and neurons that did not (Arc-). Spine densities for each region are

indicated by the branch with multiple spines in the upper part of each panel, and spine morphological subtypes are indicated by corresponding shapes (thin, subby, mushroom) in each panel. (A) Densities of mushroom spines are increased in Arc+ neurons during sleep following initial contextual fear learning. (B) Surface area, volume head, and neck length of Arc+ thin spines are increased during sleep, whereas head and neck length of mushroom spines is increased in Arc- branches. (C) Densities of Arc+ mushroom spines and Arc- thin and mushroom spines are increased during sleep following re-exposure to fear conditioning 28 days after the initial exposure. (D) Volume and head diameter of Arc+ mushroom spines is increased during sleep following re-exposure to fear conditioning, along with decreased neck length indicating strengthening of these synapses. Broad morphological changes also occur in Arc- spines during sleep suggesting more complex remodeling in these spines during sleep following re-exposure to a traumatic event. Figures 8a (Created in BioRender. Gisabella, B. (2025) https://BioRender.com/v5y092f) and 8b (Created in BioRender. Gisabella, B. (2025) https://BioRender.com/f36e816) were created using BioRender.

References:

1. Stickgold, R. Sleep-dependent memory consolidation. *Nature* **437**, 1272–1278 (2005).
2. Tononi, G. & Cirelli, C. Sleep and the price of plasticity: from synaptic and cellular homeostasis to memory consolidation and integration. *Neuron* **81**, 12–34 (2014).
3. Tononi, G. & Cirelli, C. Sleep function and synaptic homeostasis. *Sleep medicine reviews* **10**, 49–62 (2006).
4. Maret, S., Faraguna, U., Nelson, A.B., Cirelli, C. & Tononi, G. Sleep and waking modulate spine turnover in the adolescent mouse cortex. *Nat Neurosci* **14**, 1418–1420 (2011).
5. de Vivo, L.*, et al.* Ultrastructural evidence for synaptic scaling across the wake/sleep cycle. *Science* **355**, 507–510 (2017).
6. Cirelli, C. A molecular window on sleep: changes in gene expression between sleep and wakefulness. *The Neuroscientist : a review journal bringing neurobiology, neurology and psychiatry* **11**, 63–74 (2005).
7. Vecsey, C.G.*, et al.* Sleep deprivation impairs cAMP signalling in the hippocampus. *Nature*

461, 1122–1125 (2009).
8. Havekes, R.*, et al.* Sleep deprivation causes memory deficits by negatively impacting neuronal connectivity in hippocampal area CA1. *eLife* **5**(2016).
9. Yang, G.*, et al.* Sleep promotes branch-specific formation of dendritic spines after learning. *Science* **344**, 1173–1178 (2014).
10. Renouard, L.*, et al.* REM sleep promotes bidirectional plasticity in developing visual cortex in vivo. *Neurobiol Sleep Circadian Rhythms* **12**, 100076 (2022).
11. Zhou, Y.*, et al.* REM sleep promotes experience-dependent dendritic spine elimination in the mouse cortex. *Nature communications* **11**, 4819 (2020).
12. Li, W., Ma, L., Yang, G. & Gan, W.B. REM sleep selectively prunes and maintains new synapses in development and learning. *Nat Neurosci* **20**, 427–437 (2017).
13. Adler, A.*, et al.* Sleep promotes the formation of dendritic filopodia and spines near learning-inactive existing spines. *Proc Natl Acad Sci U S A* **118**(2021).
14. Rasch, B. & Born, J. About sleep's role in memory. *Physiol Rev* **93**, 681–766 (2013).
15. Dudai, Y., Karni, A. & Born, J. The Consolidation and Transformation of Memory. *Neuron* **88**, 20–32 (2015).
16. Perusini, J.N.*, et al.* Optogenetic stimulation of dentate gyrus engrams restores memory in Alzheimer's disease mice. *Hippocampus* (2017).
17. Cazzulino, A.S., Martinez, R., Tomm, N.K. & Denny, C.A. Improved specificity of hippocampal memory trace labeling. *Hippocampus* **26**, 752–762 (2016).
18. Root, C.M., Denny, C.A., Hen, R. & Axel, R. The participation of cortical amygdala in innate, odour-driven behaviour. *Nature* **515**, 269–273 (2014).
19. Denny, C.A.*, et al.* Hippocampal memory traces are differentially modulated by experience, time, and adult neurogenesis. *Neuron* **83**, 189–201 (2014).
20. Cohen, S., Kaplan, Z., Zohar, J. & Cohen, H. Preventing sleep on the first resting phase following a traumatic event attenuates anxiety-related responses. *Behav Brain Res* **320**, 450–456 (2017).
21. Kuriyama, K., Soshi, T. & Kim, Y. Sleep deprivation facilitates extinction of implicit fear generalization and physiological response to fear. *Biol Psychiatry* **68**, 991–998 (2010).
22. Cohen, S.*, et al.* Post-exposure sleep deprivation facilitates correctly timed interactions between glucocorticoid and adrenergic systems, which attenuate traumatic stress responses. *Neuropsychopharmacology* **37**, 2388–2404 (2012).
23. Kilpatrick, D.G.*, et al.* National estimates of exposure to traumatic events and PTSD prevalence using DSM-IV and DSM-5 criteria. *Journal of traumatic stress* **26**, 537–547 (2013).
24. Breslau, N., Chilcoat, H.D., Kessler, R.C. & Davis, G.C. Previous exposure to trauma and PTSD effects of subsequent trauma: results from the Detroit Area Survey of Trauma. *Am J Psychiatry* **156**, 902–907 (1999).
25. Brewin, C.R., Andrews, B. & Valentine, J.D. Meta-analysis of risk factors for posttraumatic stress disorder in trauma-exposed adults. *Journal of consulting and clinical psychology* **68**, 748–766 (2000).
26. Scott, S.T. Multiple traumatic experiences and the development of posttraumatic stress disorder. *J Interpers Violence* **22**, 932–938 (2007).
27. Suliman, S.*, et al.* Cumulative effect of multiple trauma on symptoms of posttraumatic stress disorder, anxiety, and depression in adolescents. *Comprehensive psychiatry* **50**, 121–127 (2009).
28. Perusini, J.N.*, et al.* Optogenetic stimulation of dentate gyrus engrams restores memory in Alzheimer's disease mice. *Hippocampus* **27**, 1110–1122 (2017).
29. Rexrode, L.*, et al.* Regulation of dendritic spines in the amygdala following sleep deprivation. *Front Sleep* **2**(2023).
30. Watakabe, A.*, et al.* Comparative analyses of adeno-associated viral vector serotypes 1, 2, 5, 8 and 9 in marmoset, mouse and macaque cerebral cortex. *Neurosci Res* **93**, 144–157 (2015).
31. Whitfield, J., Littlewood, T. & Soucek, L. Tamoxifen administration to mice. *Cold Spring Harb Protoc* **2015**, 269–271 (2015).

32. Whitfield, J., Littlewood, T., Evan, G.I. & Soucek, L. The estrogen receptor fusion system in mouse models: a reversible switch. *Cold Spring Harb Protoc* **2015**, 227–234 (2015).
33. Gisabella, B.*, et al.* Growth hormone biases amygdala network activation after fear learning. *Transl Psychiatry* **6**, e960 (2016).
34. Pantazopoulos, H.*, et al.* Circadian Rhythms of Perineuronal Net Composition. *eNeuro* **7**(2020).
35. Hines, D.J., Schmitt, L.I., Hines, R.M., Moss, S.J. & Haydon, P.G. Antidepressant effects of sleep deprivation require astrocyte-dependent adenosine mediated signaling. *Transl Psychiatry* **3**, e212 (2013).
36. Burgdorf, J.S.*, et al.* NMDAR activation regulates the daily rhythms of sleep and mood. *Sleep* **42**(2019).
37. Aguilar, D.D., Strecker, R.E., Basheer, R. & McNally, J.M. Alterations in sleep, sleep spindle, and EEG power in mGluR5 knockout mice. *J Neurophysiol* **123**, 22–33 (2020).
38. Yuan, R.K.*, et al.* Differential effect of sleep deprivation on place cell representations, sleep architecture, and memory in young and old mice. *Cell Rep* **35**, 109234 (2021).
39. Gisabella, B., Scammell, T., Bandaru, S.S. & Saper, C.B. Regulation of hippocampal dendritic spines following sleep deprivation. *J Comp Neurol* **528**, 380–388 (2020).
40. Havekes, R.*, et al.* Sleep deprivation causes memory deficits by negatively impacting neuronal connectivity in hippocampal area CA1. *Elife* **5**(2016).
41. Dickstein, D.L.*, et al.* Automatic Dendritic Spine Quantification from Confocal Data with Neurolucida 360. *Curr Protoc Neurosci* **77**, 1.27.21–21.27.21 (2016).
42. Rodriguez, A., Ehlenberger, D.B., Dickstein, D.L., Hof, P.R. & Wearne, S.L. Automated three-dimensional detection and shape classification of dendritic spines from fluorescence microscopy images. *PLoS One* **3**, e1997 (2008).
43. Araya, R., Vogels, T.P. & Yuste, R. Activity-dependent dendritic spine neck changes are correlated with synaptic strength. *Proc Natl Acad Sci U S A* **111**, E2895–2904 (2014).
44. Ofer, N., Berger, D.R., Kasthuri, N., Lichtman, J.W. & Yuste, R. Ultrastructural analysis of dendritic spine necks reveals a continuum of spine morphologies. *Dev Neurobiol* **81**, 746–757 (2021).
45. Arellano, J.I., Benavides-Piccione, R., Defelipe, J. & Yuste, R. Ultrastructure of dendritic spines: correlation between synaptic and spine morphologies. *Frontiers in neuroscience* **1**, 131–143 (2007).
46. Kopec, C.D., Real, E., Kessels, H.W. & Malinow, R. GluR1 links structural and functional plasticity at excitatory synapses. *J Neurosci* **27**, 13706–13718 (2007).
47. Borczyk, M., Sliwinska, M.A., Caly, A., Bernas, T. & Radwanska, K. Neuronal plasticity affects correlation between the size of dendritic spine and its postsynaptic density. *Scientific reports* **9**, 1693 (2019).
48. Noguchi, J., Matsuzaki, M., Ellis-Davies, G.C. & Kasai, H. Spine-neck geometry determines NMDA receptor-dependent Ca2+ signaling in dendrites. *Neuron* **46**, 609–622 (2005).
49. Harris, K.M. & Stevens, J.K. Dendritic spines of CA 1 pyramidal cells in the rat hippocampus: serial electron microscopy with reference to their biophysical characteristics. *J Neurosci* **9**, 2982–2997 (1989).
50. Spano, G.M.*, et al.* Sleep Deprivation by Exposure to Novel Objects Increases Synapse Density and Axon-Spine Interface in the Hippocampal CA1 Region of Adolescent Mice. *J Neurosci* **39**, 6613–6625 (2019).
51. Wang, L.*, et al.* Sleep-dependent engram reactivation during hippocampal memory consolidation associated with subregion-specific biosynthetic changes. *iScience* **27**, 109408 (2024).
52. Lai, K.O., Liang, Z., Fei, E., Huang, H. & Ip, N.Y. Cyclin-dependent Kinase 5 (Cdk5)-dependent Phosphorylation of p70 Ribosomal S6 Kinase 1 (S6K) Is Required for Dendritic Spine Morphogenesis. *J Biol Chem* **290**, 14637–14646 (2015).
53. Puighermanal, E.*, et al.* Ribosomal Protein S6 Phosphorylation Is Involved in Novelty-Induced Locomotion, Synaptic Plasticity and mRNA Translation. *Frontiers in molecular neuroscience* **10**, 419 (2017).
54. Eyries, M., Agrapart, M., Alonso, A. & Soubrier, F. Phorbol ester induction of angiotensin-

converting enzyme transcription is mediated by Egr-1 and AP-1 in human endothelial cells via ERK1/2 pathway. *Circulation research* **91**, 899–906 (2002).
55. Medina, J.H. & Viola, H. ERK1/2: A Key Cellular Component for the Formation, Retrieval, Reconsolidation and Persistence of Memory. *Frontiers in molecular neuroscience* **11**, 361 (2018).
56. Lee, C.*, et al.* Hippocampal engram networks for fear memory recruit new synapses and modify pre-existing synapses in vivo. *Curr Biol* **33**, 507–516 e503 (2023).
57. Gobbo, F.*, et al.* Distinct spatial distribution of potentiated dendritic spines in encoding- and recall-activated hippocampal neurons. *Frontiers in molecular neuroscience* **Volume 18 - 2025**(2026).
58. Spruston, N. & McBain, C.J. Structural and Functional Properties of Hippocampal Neurons. in *The Hippocampus Book* (eds. Andersen, P., Morris, R., Amaral, D.G., Bliss, T.V. & O' Keefe, J.) 133–201 (Oxford Scholarship Online, 2006).
59. Remaud, J.*, et al.* Anisomycin injection in area CA3 of the hippocampus impairs both short-term and long-term memories of contextual fear. *Learn Mem* **21**, 311–315 (2014).
60. Daumas, S., Ceccom, J., Halley, H., Frances, B. & Lassalle, J.M. Activation of metabotropic glutamate receptor type 2/3 supports the involvement of the hippocampal mossy fiber pathway on contextual fear memory consolidation. *Learn Mem* **16**, 504–507 (2009).
61. Choi, J.H.*, et al.* Interregional synaptic maps among engram cells underlie memory formation. *Science* **360**, 430–435 (2018).
62. Choi, D.I.*, et al.* Synaptic correlates of associative fear memory in the lateral amygdala. *Neuron* **109**, 2717–2726 e2713 (2021).
63. Bourne, J. & Harris, K.M. Do thin spines learn to be mushroom spines that remember? *Curr Opin Neurobiol* **17**, 381–386 (2007).
64. Kasai, H., Matsuzaki, M., Noguchi, J., Yasumatsu, N. & Nakahara, H. Structure-stability-function relationships of dendritic spines. *Trends Neurosci* **26**, 360–368 (2003).
65. Maletic-Savatic, M., Malinow, R. & Svoboda, K. Rapid dendritic morphogenesis in CA1 hippocampal dendrites induced by synaptic activity. *Science* **283**, 1923–1927 (1999).
66. Engert, F. & Bonhoeffer, T. Dendritic spine changes associated with hippocampal long-term synaptic plasticity. *Nature* **399**, 66–70 (1999).
67. Tominaga-Yoshino, K., Urakubo, T., Okada, M., Matsuda, H. & Ogura, A. Repetitive induction of late-phase LTP produces long-lasting synaptic enhancement accompanied by synaptogenesis in cultured hippocampal slices. *Hippocampus* **18**, 281–293 (2008).
68. Graves, L.A., Heller, E.A., Pack, A.I. & Abel, T. Sleep deprivation selectively impairs memory consolidation for contextual fear conditioning. *Learn Mem* **10**, 168–176 (2003).
69. Foilb, A.R., Taylor-Yeremeeva, E.M., Schmidt, B.D., Ressler, K.J. & Carlezon, W.A., Jr. Acute sleep disruption reduces fear memories in male and female mice. *Neuropsychopharmacology* **50**, 401–409 (2024).
70. Lommen, M.J.J., Hoekstra, S., van den Brink, R.H.S. & Lenaert, B. Fear generalization predicts post-traumatic stress symptoms: A two-year follow-up study in Dutch fire fighters. *Journal of anxiety disorders* **103**, 102855 (2024).
71. Kaczkurkin, A.N.*, et al.* Neural Substrates of Overgeneralized Conditioned Fear in PTSD. *Am J Psychiatry* **174**, 125–134 (2017).
72. Wagner, U., Hallschmid, M., Rasch, B. & Born, J. Brief sleep after learning keeps emotional memories alive for years. *Biol Psychiatry* **60**, 788–790 (2006).
73. Baczynska, E., Pels, K.K., Basu, S., Wlodarczyk, J. & Ruszczycki, B. Quantification of Dendritic Spines Remodeling under Physiological Stimuli and in Pathological Conditions. *International journal of molecular sciences* **22**(2021).
74. Ofer, N., Benavides-Piccione, R., DeFelipe, J. & Yuste, R. Structural Analysis of Human and Mouse Dendritic Spines Reveals a Morphological Continuum and Differences across Ages and Species. *eNeuro* **9**(2022).
75. Yap, K.*, et al.* The actin-modulating protein synaptopodin mediates long-term survival of dendritic spines. *eLife* **9**(2020).
76. Vazdarjanova, A.*, et al.* Spatial exploration induces ARC, a plasticity-related immediate-early gene, only in calcium/calmodulin-dependent protein kinase II-positive principal

excitatory and inhibitory neurons of the rat forebrain. *J Comp Neurol* **498**, 317–329 (2006).
77. Raven, F.*, et al.* Brief sleep disruption alters synaptic structures among hippocampal and neocortical somatostatin-expressing interneurons. *Sleep* **48**(2025).
78. Delorme, J.*, et al.* Sleep loss drives acetylcholine- and somatostatin interneuron-mediated gating of hippocampal activity to inhibit memory consolidation. *Proc Natl Acad Sci U S A* **118**(2021).
79. Steward, O., Wallace, C.S., Lyford, G.L. & Worley, P.F. Synaptic activation causes the mRNA for the IEG Arc to localize selectively near activated postsynaptic sites on dendrites. *Neuron* **21**, 741–751 (1998).
80. Morin, J.P., Guzman-Ramos, K. & Bermudez-Rattoni, F. New Insights on Retrieval-Induced and Ongoing Memory Consolidation: Lessons from Arc. *Neural plasticity* **2015**, 184083 (2015).

Figure 1

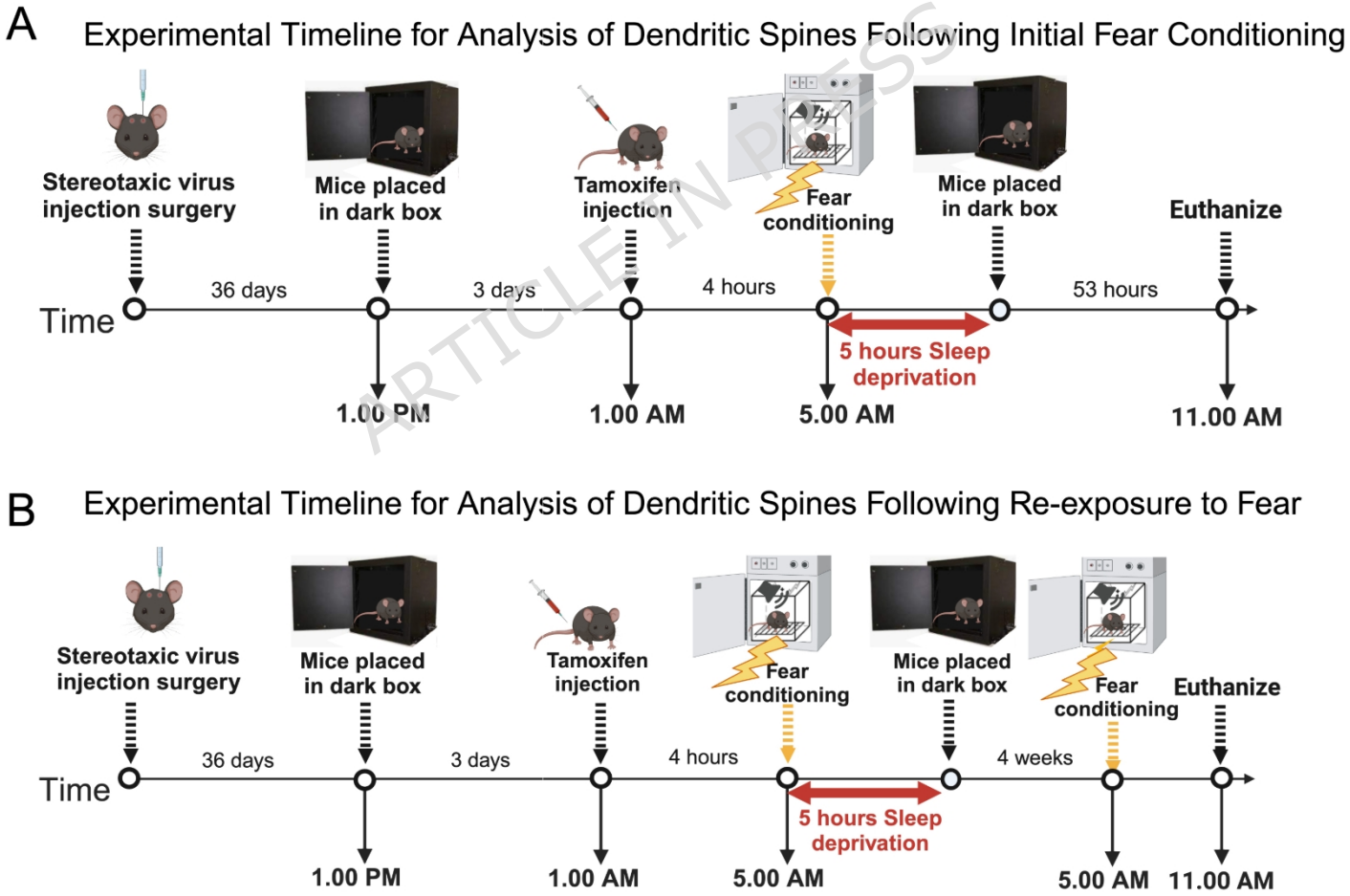

Figure 2

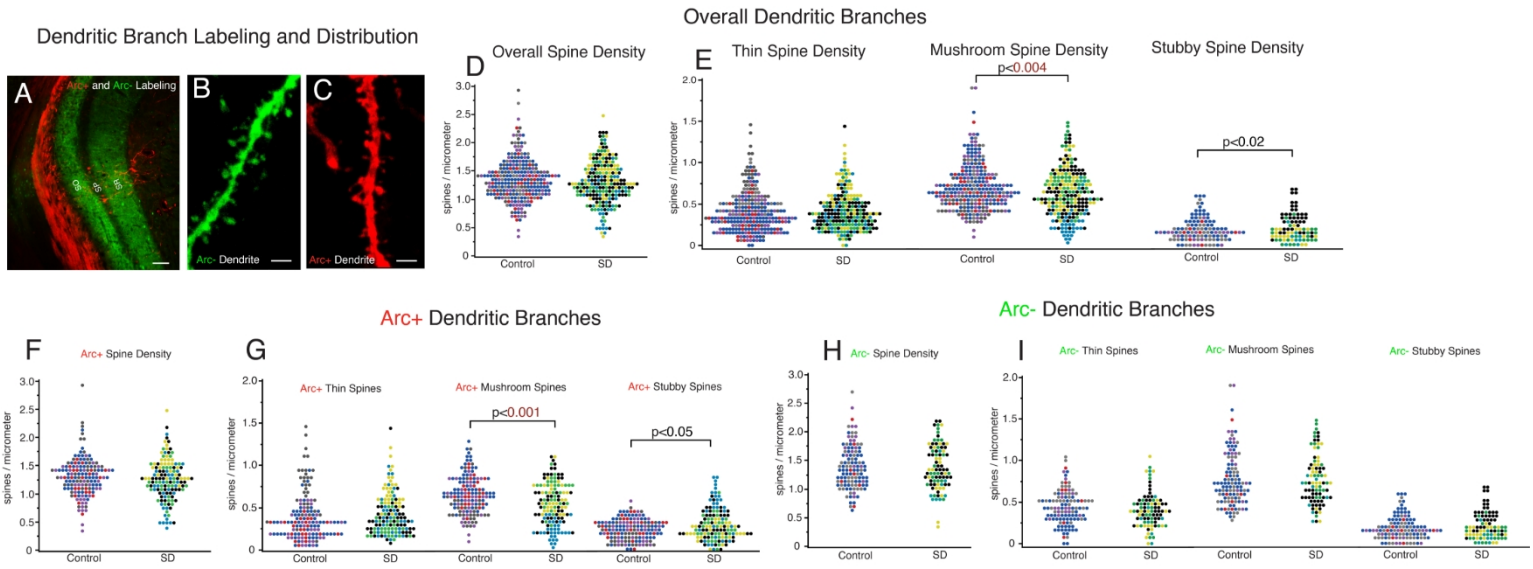

Figure 3

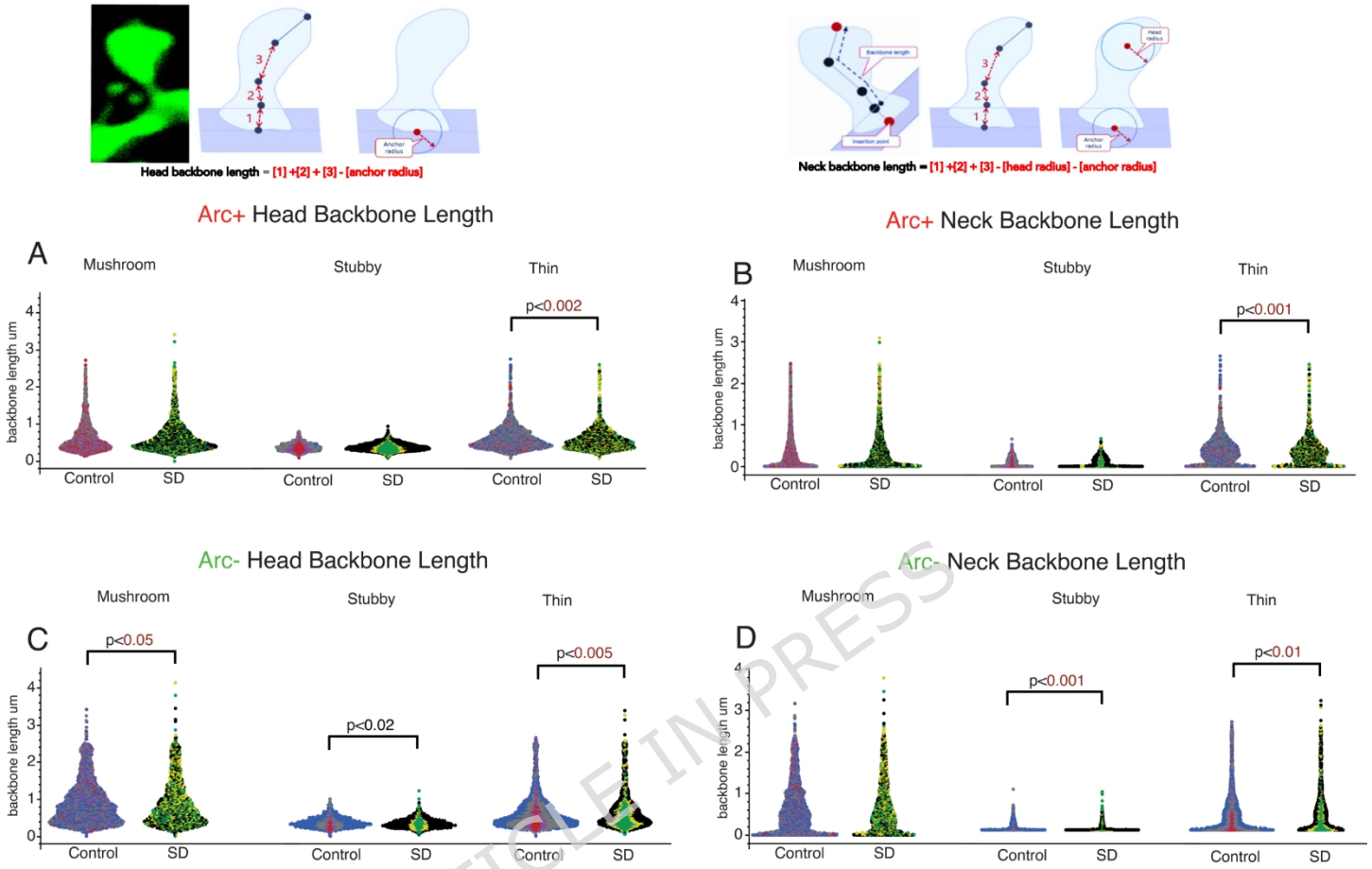

Figure 4

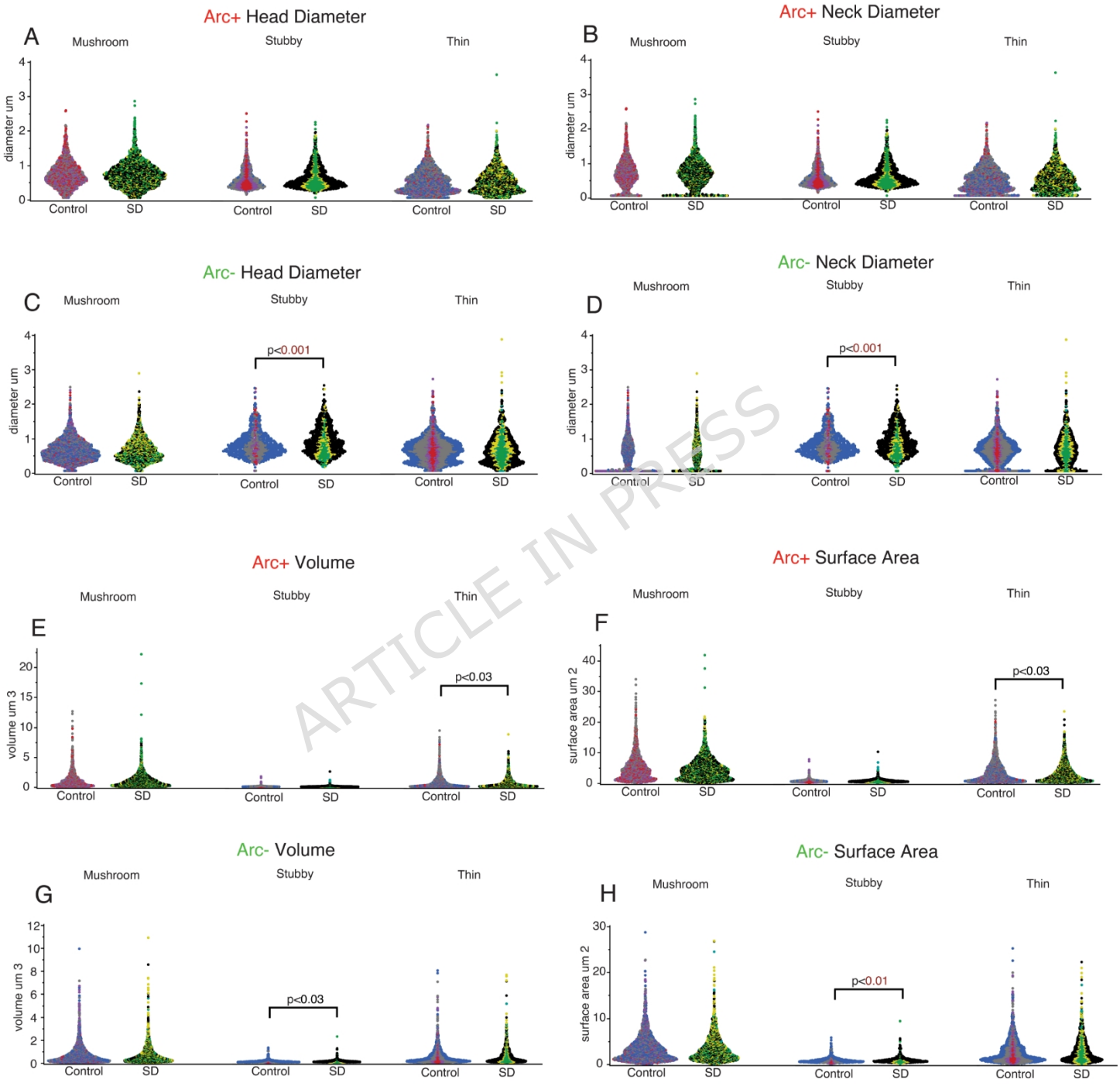

Figure 5

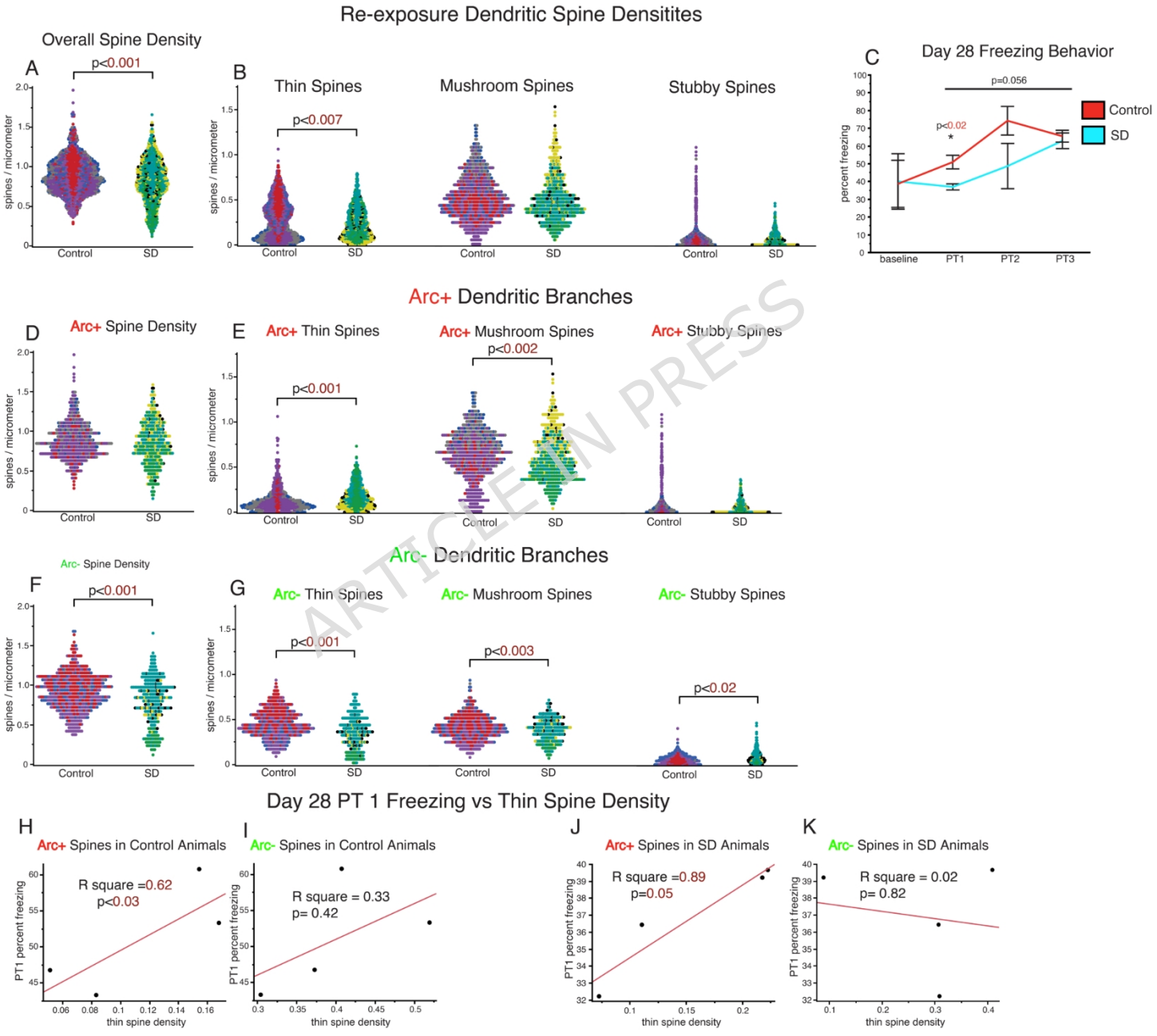

Figure 6

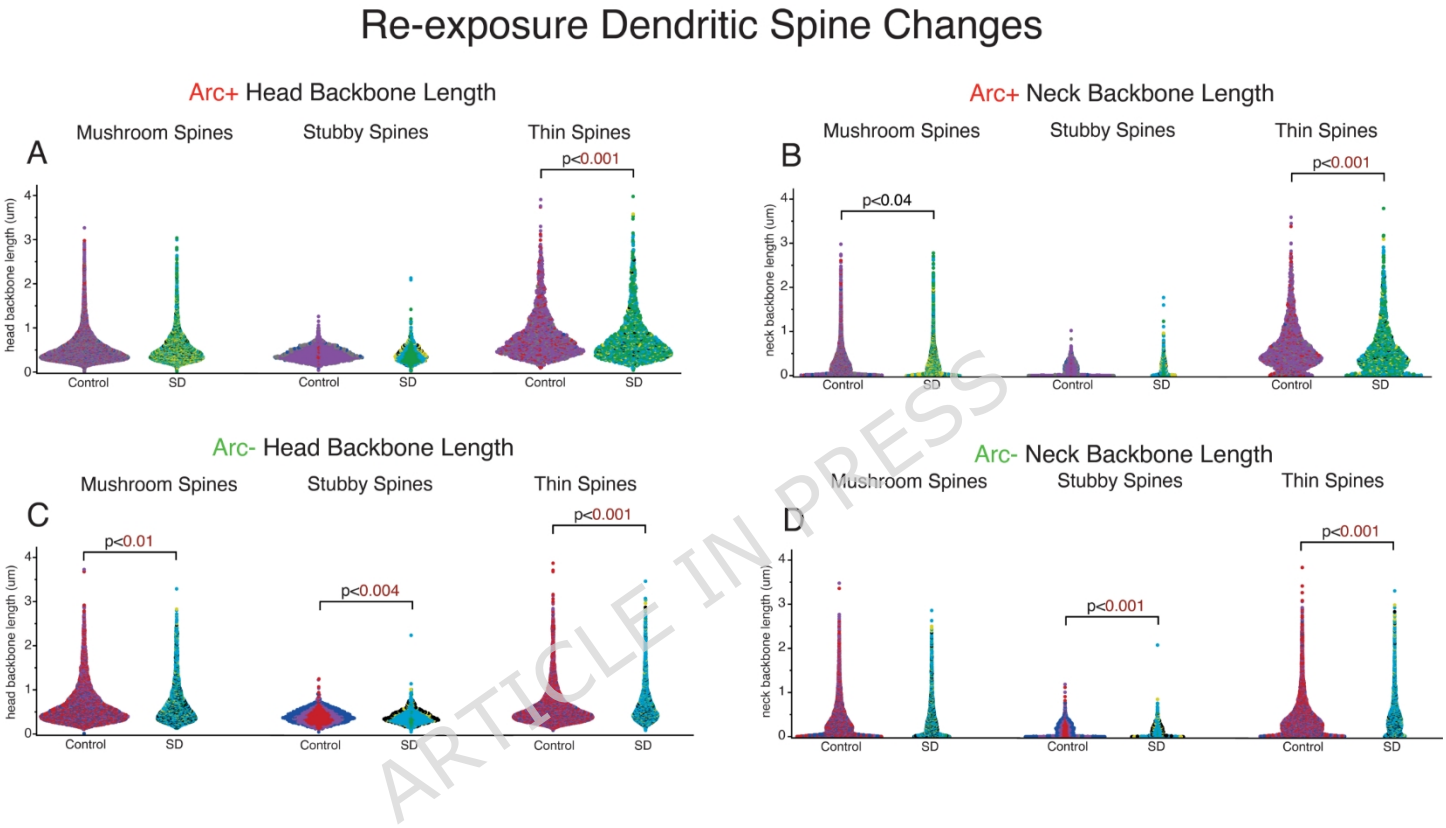

Figure 7

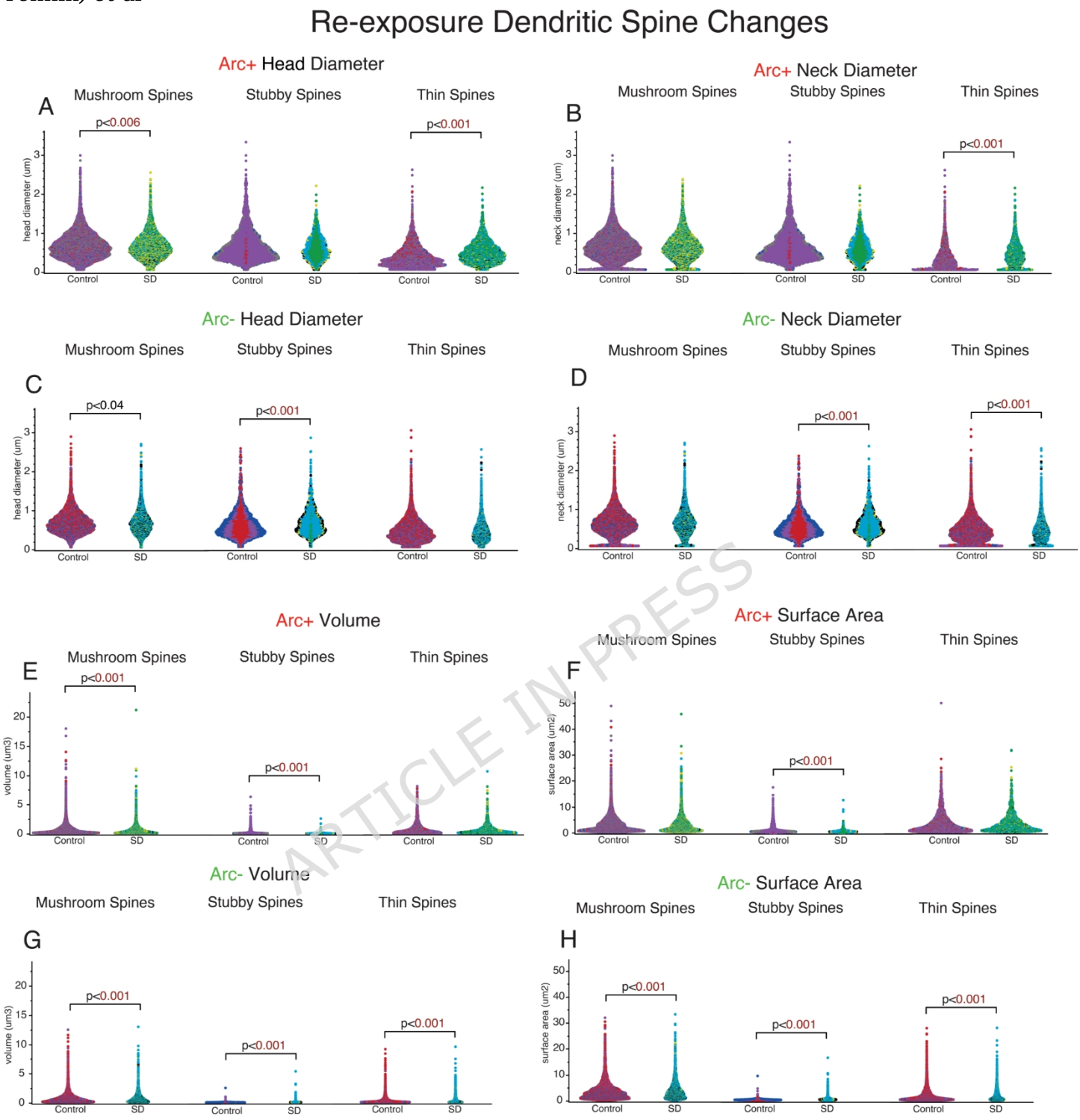

Figure 8

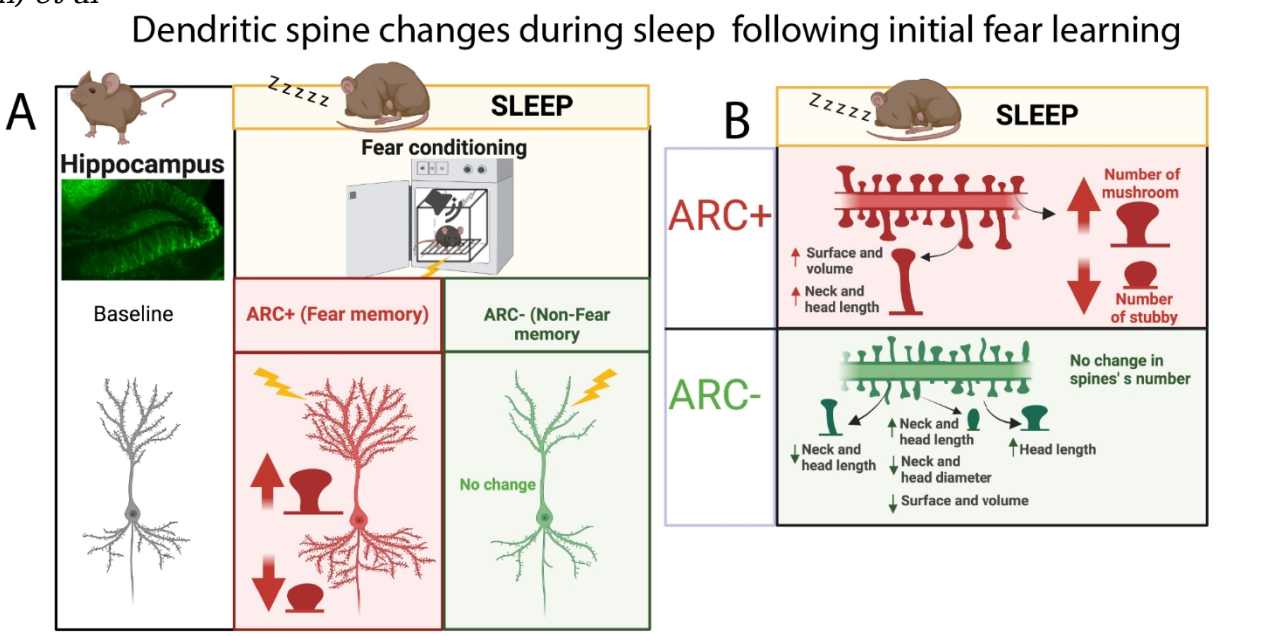

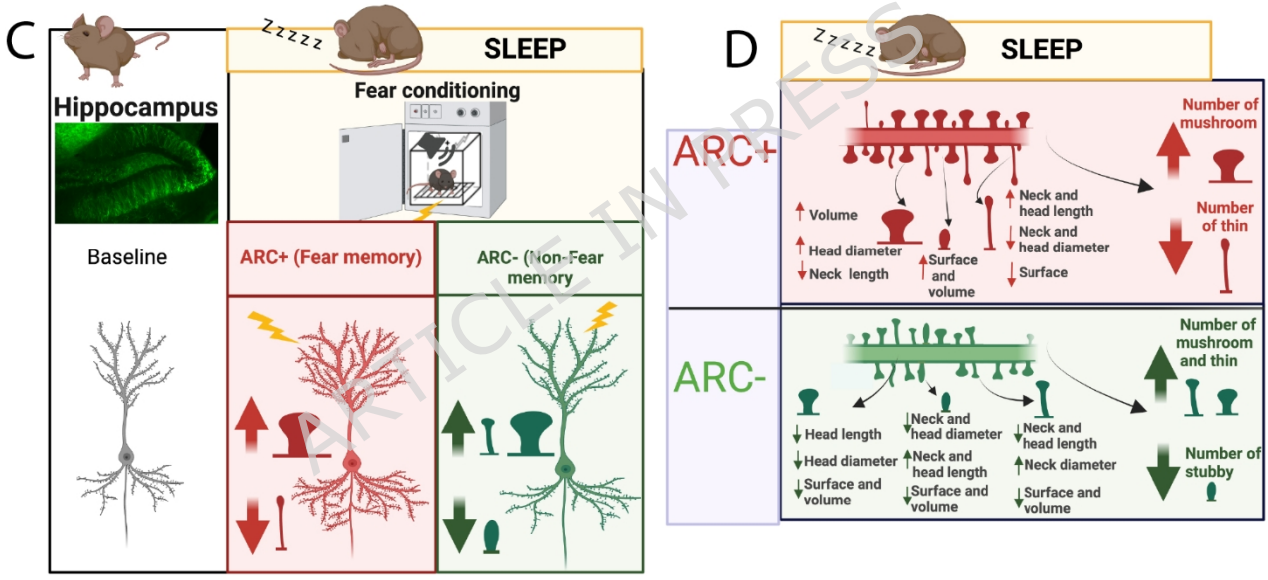

A Experimental Timeline for Analysis of Dendritic Spines Following Initial Fear Conditioning

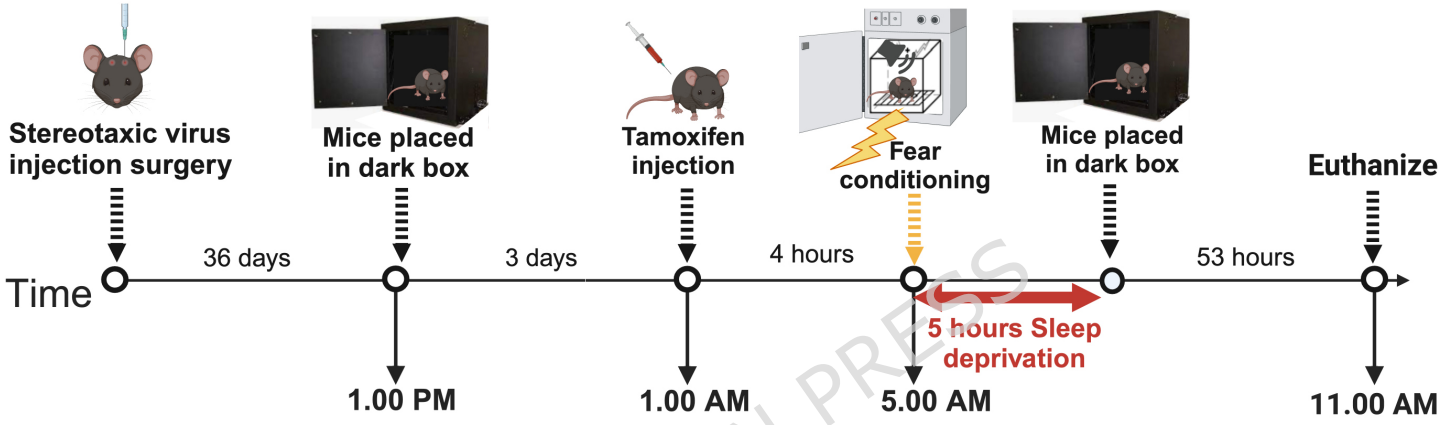

B Experimental Timeline for Analysis of Dendritic Spines Following Re-exposure to Fear

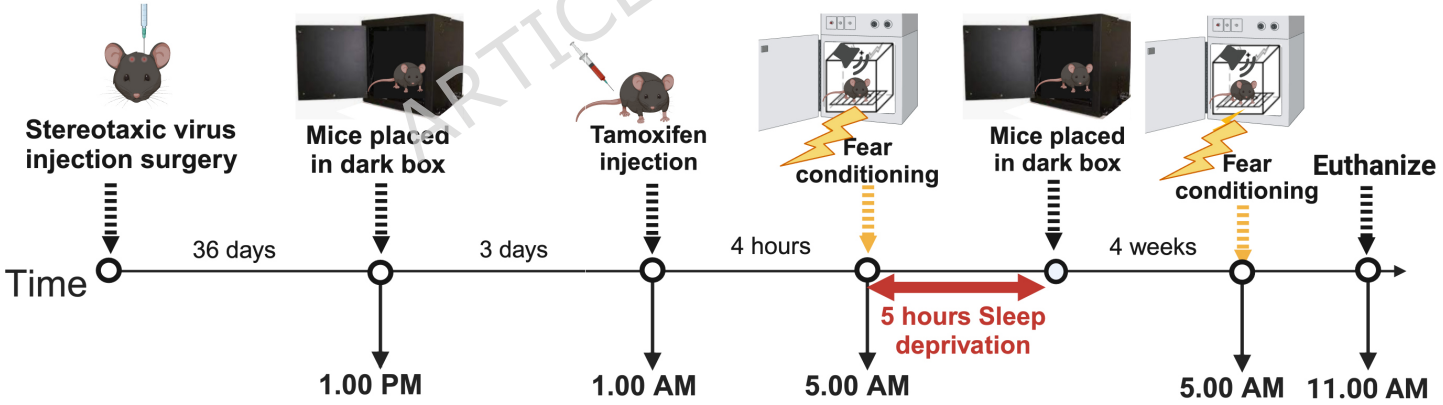

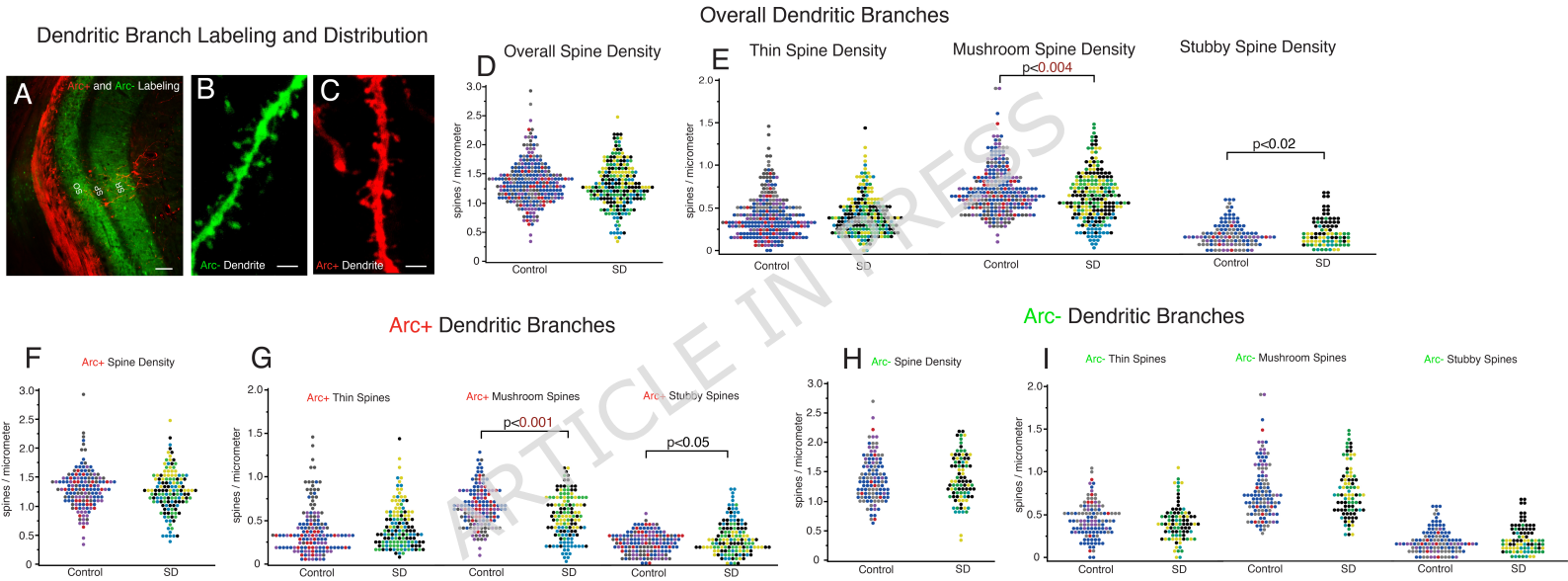

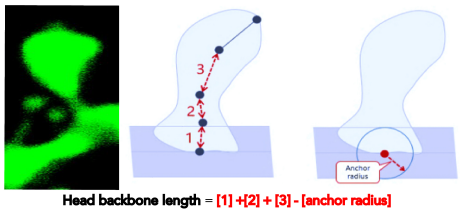

Head backbone length = [1] +[2] + [3] - [anchor radius]

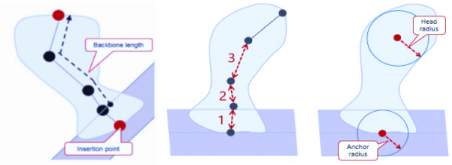

Neck backbone length = [1] +[2] + [3] - [head radius] - [anchor radius]

Arc+ Head Backbone Length

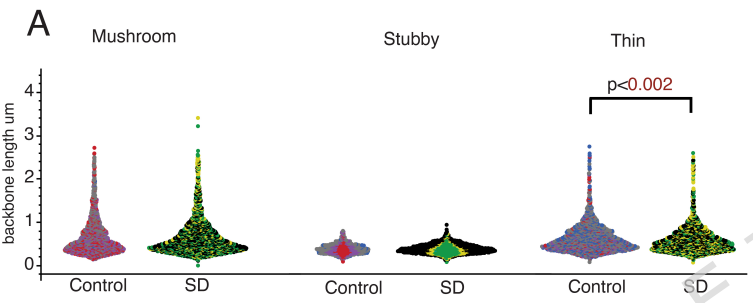

Arc+ Neck Backbone Length

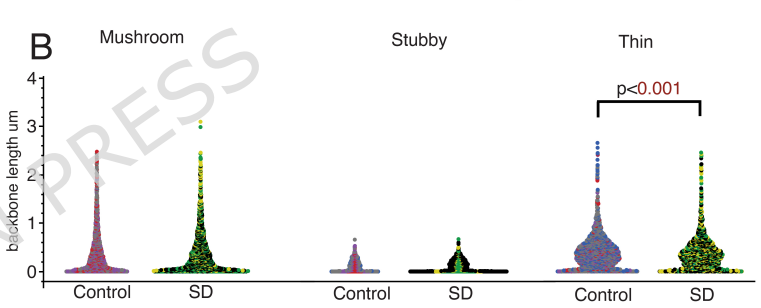

Arc- Head Backbone Length

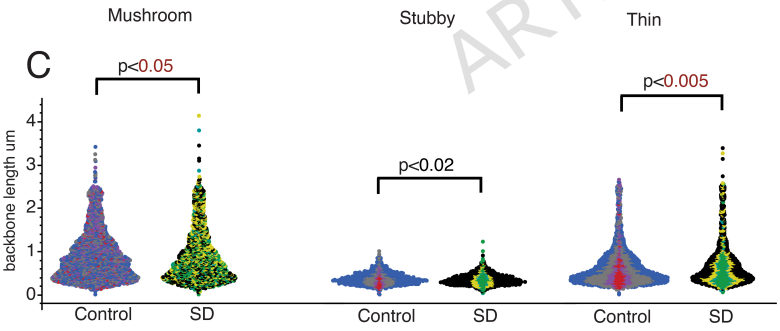

Arc- Neck Backbone Length

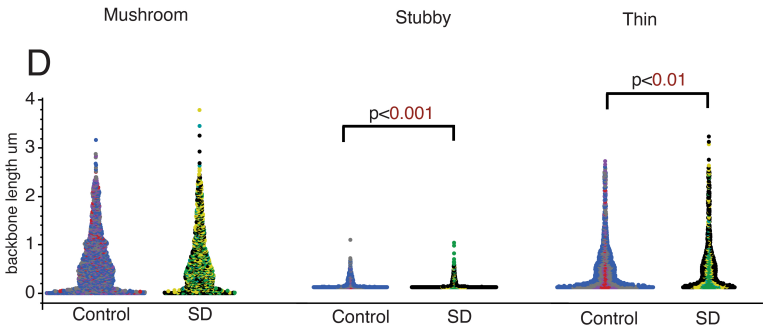

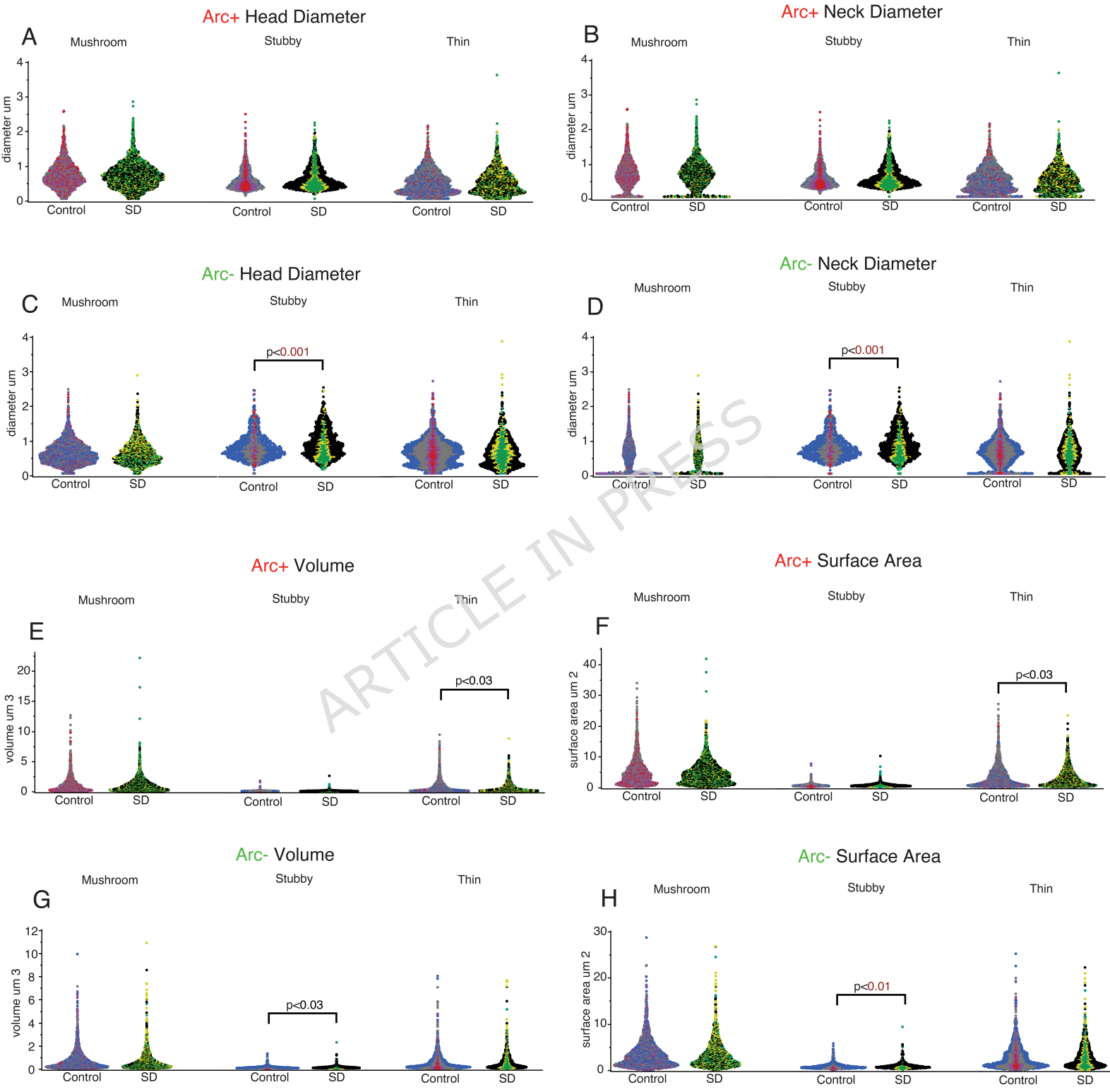

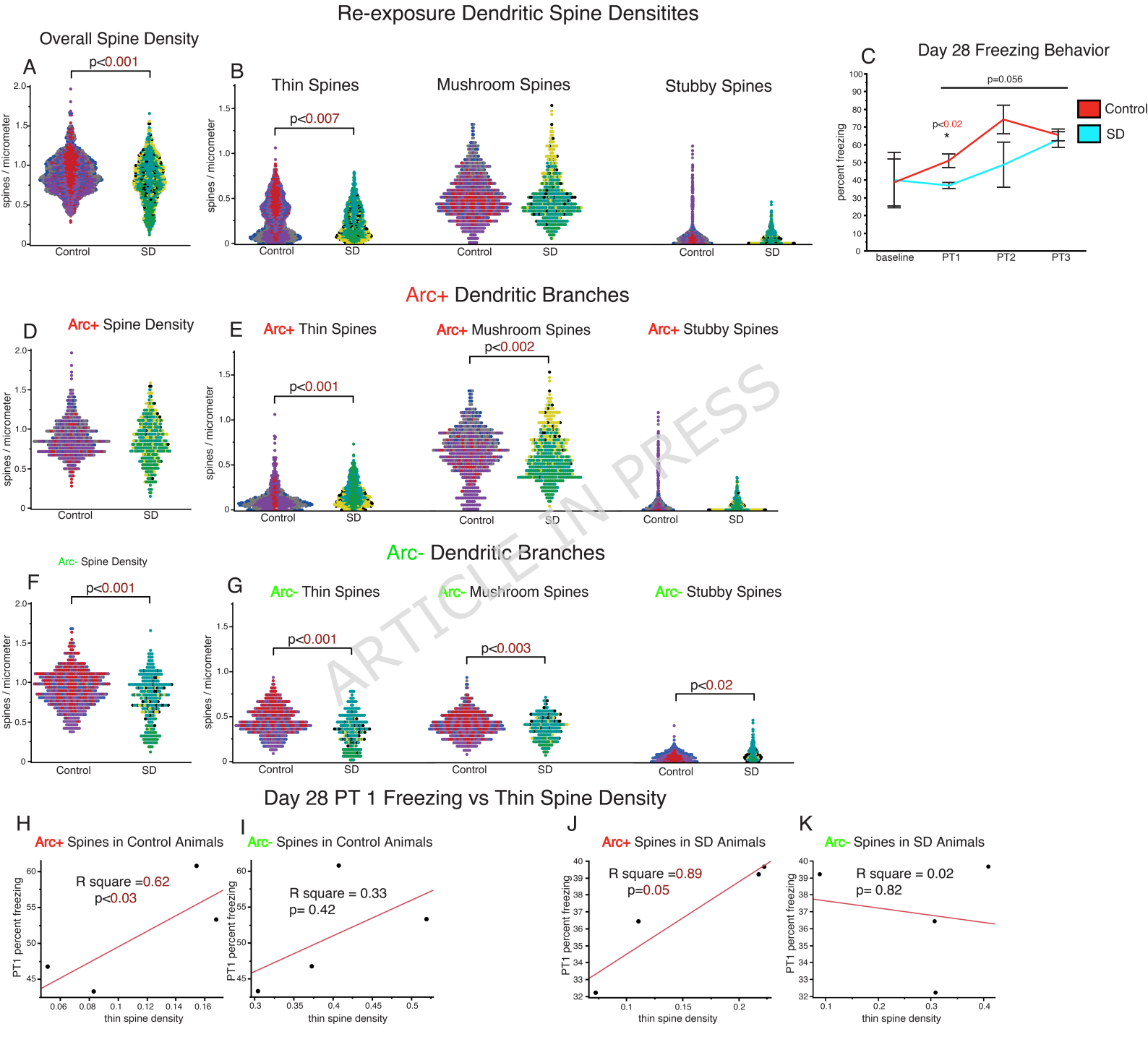

Re-exposure Dendritic Spine Changes

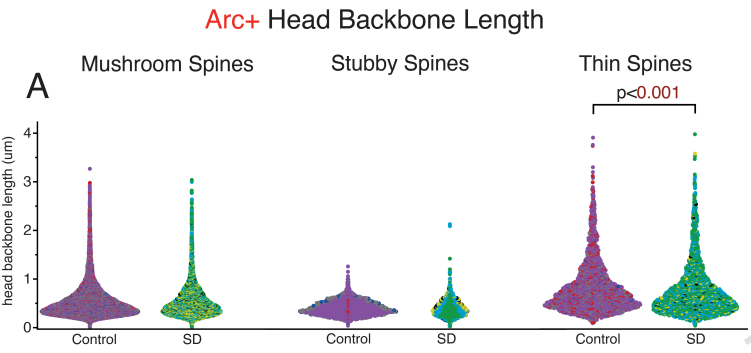

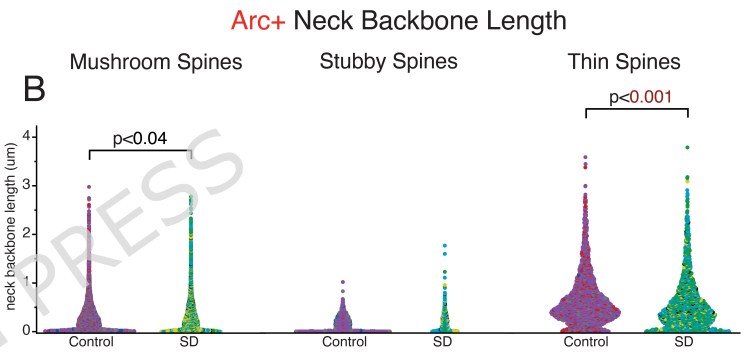

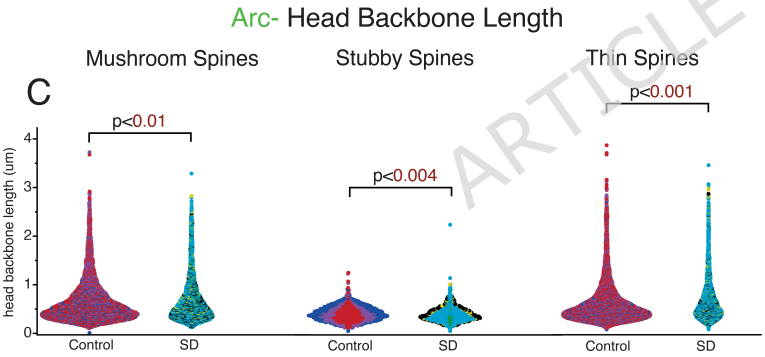

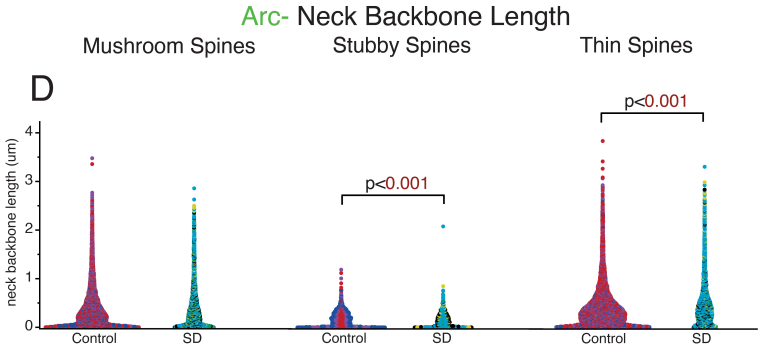

Re-exposure Dendritic Spine Changes

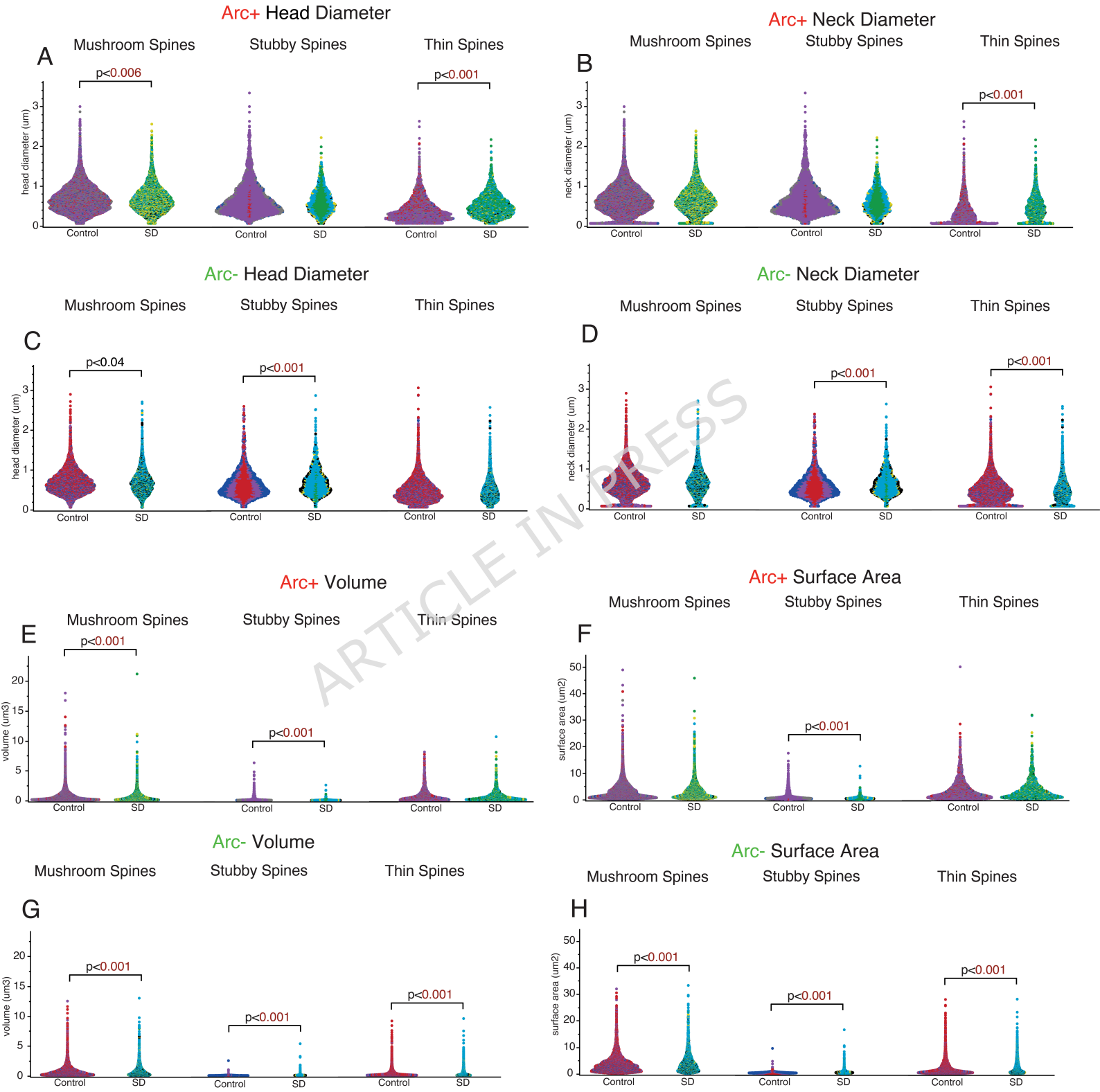

Dendritic spine changes during sleep following initial fear learning

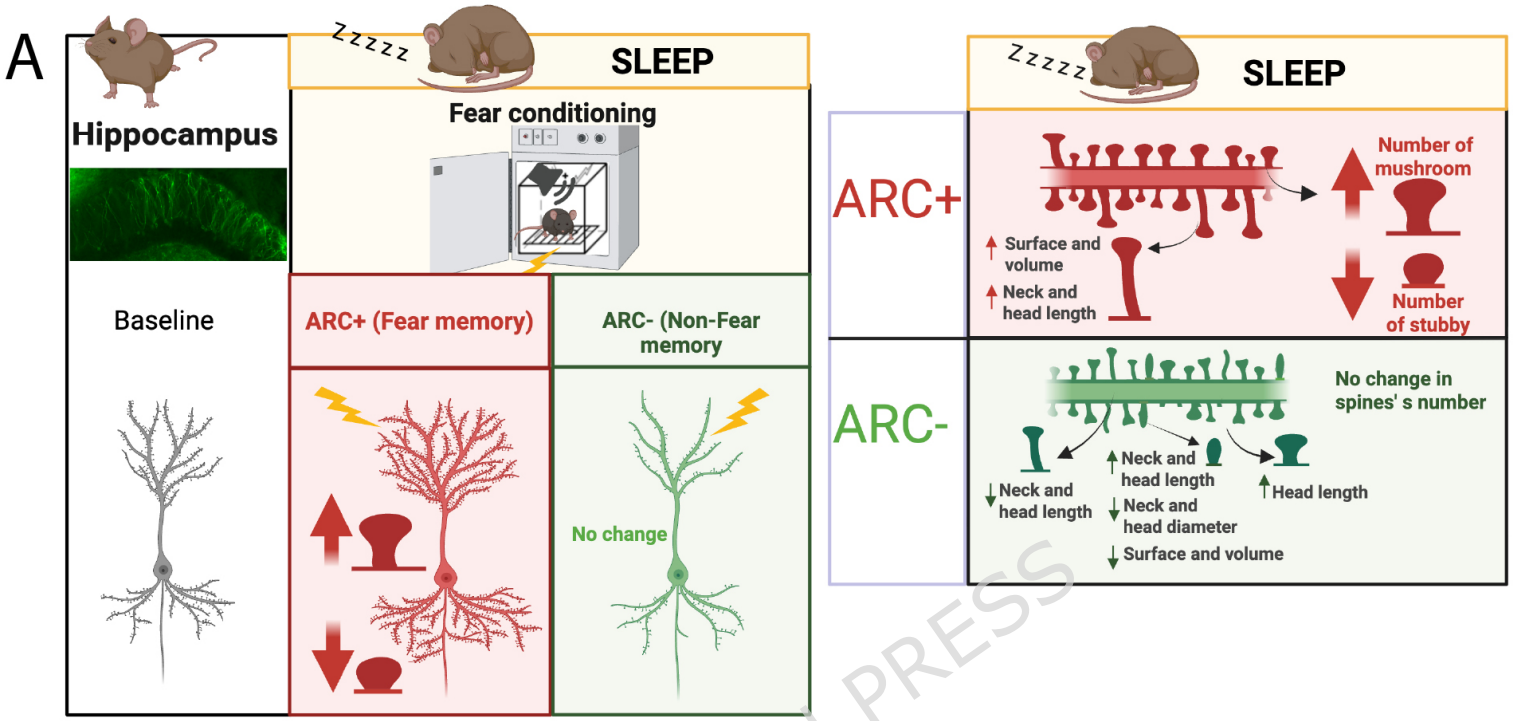

Dendritic spine changes during sleep following fear re-exposure 28 days later